

CELL BIOLOGY

CD13 tethers the IQGAP1-ARF6-EFA6 complex to the plasma membrane to promote ARF6 activation, β 1 integrin recycling, and cell migration

Mallika Ghosh*, Robin Lo, Ivan Ivic, Brian Aguilera, Veneta Qendro, Charan Devarakonda, Linda H. Shapiro*

Copyright © 2019
The Authors, some
rights reserved;
exclusive licensee
American Association
for the Advancement
of Science. No claim
to original U.S.
Government Works

Cell attachment to the extracellular matrix (ECM) requires a balance between integrin internalization and recycling to the surface that is mediated by numerous proteins, emphasizing the complexity of these processes. Upon ligand binding in various cells, the β 1 integrin is internalized, traffics to early endosomes, and is returned to the plasma membrane through recycling endosomes. This trafficking process depends on the cyclical activation and inactivation of small guanosine triphosphatases (GTPases) by their specific guanine exchange factors (GEFs) and their GTPase-activating proteins (GAPs). In this study, we found that the cell surface antigen CD13, a multifunctional transmembrane molecule that regulates cell-cell adhesion and receptor-mediated endocytosis, also promoted cell migration and colocalized with β 1 integrin at sites of cell adhesion and at the leading edge. A lack of CD13 resulted in aberrant trafficking of internalized β 1 integrin to late endosomes and its ultimate degradation. Our data indicate that CD13 promoted ARF6 GTPase activity by positioning the ARF6-GEF EFA6 at the cell membrane. In migrating cells, a complex containing phosphorylated CD13, IQGAP1, GTP-bound (active) ARF6, and EFA6 at the leading edge promoted the ARF6 GTPase cycling and cell migration. Together, our findings uncover a role for CD13 in the fundamental cellular processes of receptor recycling, regulation of small GTPase activities, cell-ECM interactions, and cell migration.

INTRODUCTION

Cell communication with the extracellular environment is a universal property shared by distinct cell types that underlies many normal biological processes, such that absent or dysregulated connections can give rise to aberrant and sometimes lethal consequences. At sites of interaction, cells form complexes containing hundreds of proteins of diverse classes that link the cytoskeleton to the plasma membrane and the extracellular matrix (ECM). These trigger signal transduction cascades to mediate the cytoskeletal rearrangements necessary for cellular functions such as shape change and motility (1, 2). A critical step in this process is the endocytic internalization and recycling of components of these complexes, particularly the integrin molecules that connect their ECM ligands to the actin cytoskeleton (3). These processes are controlled by families of small guanosine triphosphatases (GTPases) [adenosine diphosphate ribosylation factors (ARFs), Rabs, etc.], their regulators, GTPase-activating proteins (GAPs), and guanine exchange factors (GEFs) (4) that trigger the activation of Rho-GTPase signaling cascades and their numerous effectors (5). Pertinent to this study, the cyclic activation and inactivation of the type III ARF, ARF6, mediates β 1 integrin endocytic internalization, subsequent endosomal trafficking, recycling to the membrane, and, last, fusion with the plasma membrane, thus controlling cell-ECM adhesion and migration by integrin availability (6). Blocking or inhibiting ARF6 activation abrogates β 1 integrin recycling and consequent cell migration (7, 8). Subsequent ARF6 activities are directed by various effector molecules and scaffolding proteins. For example, the active form of the GTPase Rab35 recruits the ARF6-GAP ACAP2 to inactivate ARF6 and block β 1 integrin recycling (9),

Rab5c-induced formation of an ARF6-AMAP1- β 1 integrin complex promotes β 1 integrin recycling and cell motility (10), whereas the ARF6-Rac1-IQ motif-containing GAP 1 (IQGAP1) complex is required for tumor cell migration (7). Pertinent to our study, these complexes must be correctly positioned within the cell to carry out their functions (7, 8). Although such communication complexes have been studied for many years in numerous cell types, the wealth of new reports identifying associated proteins, interactions, and functions emphasizes the fact that important questions remain regarding the regulation of the interactions and organization of these proteins and their subsequent signaling pathways.

We have previously demonstrated that the multifunctional transmembrane peptidase CD13 participates in many activities that are fundamental to cell adhesion and motility. In myeloid and endothelial cells, CD13 is a regulator of receptor-mediated endocytosis and subsequent endocytic signal transduction pathways (11–13). In addition, we have shown that CD13 is an inflammatory adhesion molecule (14–17) that also regulates endothelial cell migration by promoting Cdc42 activation and filopodia formation during angiogenesis (11, 18), prompting the current investigation into potential CD13-mediated mechanisms regulating cell-ECM interactions. We focused our study on the well-characterized β 1 integrin-fibronectin (FN) interaction and trafficking processes and demonstrated that CD13 expression promoted cell adhesion, spreading, and migration in wild-type (WT) and CD13^{KO} murine fibroblasts, the human KS1767 Kaposi sarcoma (KS) endothelial cell line engineered to delete CD13 by CRISPR technology (15), and human epithelial cells engineered to express WT but not inactive human CD13 (HCD13). In addition, whereas surface β 1 integrin was internalized and recycled back to the surface in WT cells in response to ligand, β 1 integrin was retained in intracellular vesicles in cells lacking CD13, suggesting that CD13 contributes specifically to β 1 integrin recycling. Mechanistically, we show that a complex

Center for Vascular Biology, Department of Cell Biology, University of Connecticut School of Medicine, Farmington, CT 06032, USA.

*Corresponding author. Email: mghosh@uchc.edu (M.G.); lshapiro@uchc.edu (L.H.S.)

containing active WT CD13, $\beta 1$ integrin, and its recycling coordinators active ARF6, the ARF6-specific exchange factor EFA6, and IQGAP1 localizes with F-actin at the leading edge of migrating cells and is required to maintain ARF6 in its active guanine triphosphate (GTP)-bound state. Therefore, CD13 tethers EFA6 at the cell membrane with IQGAP1 and ARF6 to activate ARF6, which is essential for proper $\beta 1$ integrin endosomal trafficking and thus is a critical regulator of cell-ECM interactions.

RESULTS

CD13 contributes to processes required for cell migration

We have previously demonstrated that CD13 functions as an inflammatory adhesion molecule on migrating monocytes (15–17, 19) that also regulates endothelial cell migration through the ECM during angiogenesis (11, 18), leading us to investigate potential CD13-mediated mechanisms regulating cell-ECM interactions and motility. Migration on the ECM involves a number of processes including cell adhesion to the substrate, cell spreading, and cell movement. Our previous studies have shown that the CD13 cytoplasmic tail is phosphorylated by the tyrosine kinase Src at Tyr⁶ in inflammatory myeloid cells, where mutation of this residue to a nonphosphorylatable Phe (CD13-Y6F) abrogates cell-cell adhesion (13, 15). To address this in ECM-adherent cells, we used WT or CD13^{KO} murine embryonic fibroblasts (MEFs) or human epithelial cells engineered to express WT HCD13, phosphorylation-defective HCD13 (Y6F), or empty vector (EV) controls in the presence of FN. These experiments

indicated that cell-ECM adhesion (Fig. 1, A and B) and relative cell spreading over time (by measuring the area circumscribed by the focal adhesion protein paxillin; Fig. 1, C and D, and fig. S1A) were markedly reduced in cells lacking CD13 or treated with the CD13-blocking antibody (Ab) SL13, as well as those expressing the mutant HCD13-Y6F compared to cells expressing WT CD13. Similarly, in an in vitro wound healing assay (Fig. 1, E and F, and fig. S1B), migration was substantially impaired over a 6-hour time period in the absence of CD13 or in cells expressing the HCD13-Y6F mutant compared to the WT counterpart. Therefore, CD13 contributes to processes necessary for cell-ECM adhesion and motility.

CD13 is important for recycling $\beta 1$ integrin to the cell surface

Cell-ECM interactions are mediated primarily by the integrin family of transmembrane adhesion proteins. The prototypic adhesion molecule $\beta 1$ integrin is activated upon binding to its ligand FN at the site of cell-ECM attachment, forming adhesion complexes that establish a tight link between the cytoskeleton and the ECM. $\beta 1$ integrin-containing adhesion complexes undergo requisite rounds of formation and disassembly, where proteins are internalized and reexpressed on the surface through highly regulated endocytic recycling mechanisms (3). We have shown that a lack of CD13 increases the internalization of some receptors upon ligand binding in myeloid and dendritic cells (12, 13), raising the possibility that CD13 promotes adhesion by maintaining $\beta 1$ integrin on the cell surface. We performed an antibody-induced pulse-chase assay in MEFs in which surface $\beta 1$ integrin is initially labeled with an

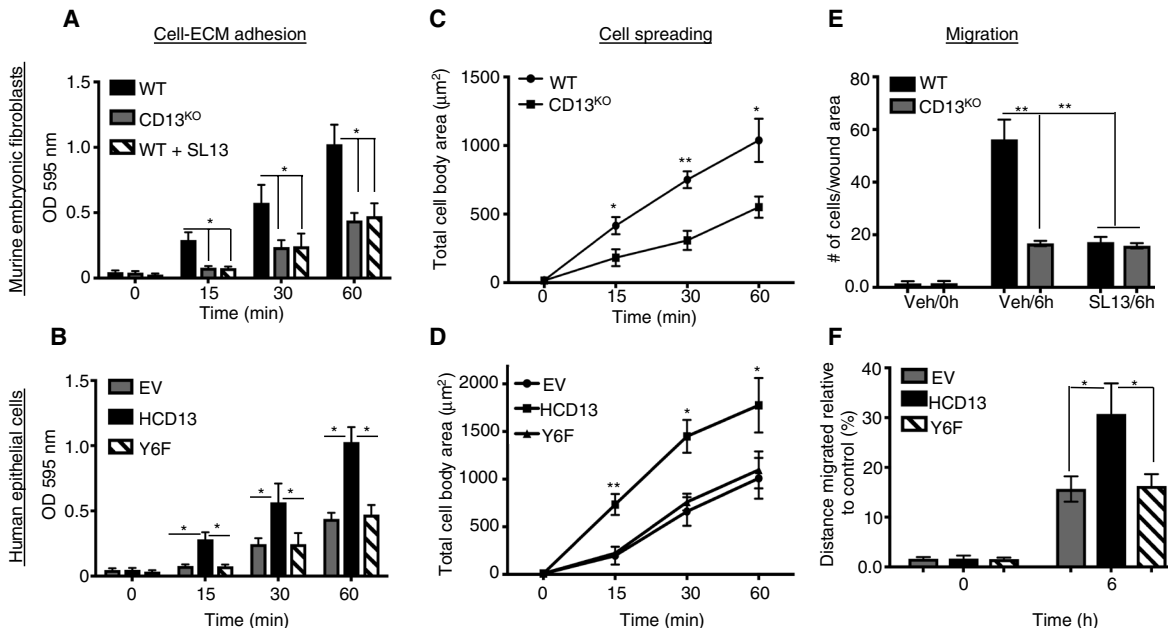


Fig. 1. Cell-ECM adhesion, cell spreading, and directional migration are substantially reduced in the absence of CD13. (A and B) Cell-ECM adhesion was assessed in MEFs [WT, CD13^{KO}, and WT treated with CD13-blocking Ab SL13; (A)] and human epithelial cells [C33A cells expressing EV, HCD13, or a phospho-tyrosine mutant CD13 (Y6F); (B)] plated in the presence of FN for the indicated time periods. Cells attached to ECM were stained with crystal violet dye, and absorbance was measured at 595 nm. OD, optical density. (C and D) Cell spreading was assessed in MEFs (C) and C33A cells (D) plated on FN and left alone to spread for the indicated time periods. Cells were then stained with antibody against paxillin and imaged using confocal microscopy. Spreading was measured in cells of similar nuclear size as the area circumscribed by paxillin staining (total cell body) using Fiji software. (E and F) Cell migration was assessed using an in vitro scratch assay, in which monolayers of MEFs (E) or C33As (F) grown on FN for 6 hours (h) were allowed to migrate into the cleared space. For MEFs, the number of cells migrating into the wound area was counted, whereas for C33A cells, the distance traveled by the leading front was measured by a phase-contrast microscopy and Fiji software. Data are means \pm SD of three independent experiments. ** $P < 0.01$ and * $P < 0.05$ by two-tailed Student's t test.

untagged anti- $\beta 1$ integrin antibody 9EG7 (recognizing ligand-bound murine integrin) in the presence of FN, followed by incubation at 37°C (pulse) to allow integrin/antibody internalization (scheme in fig. S2). After the pulse, cells were acid-stripped to remove unbound and non-internalized Abs, followed by incubation in the absence of the antibody for 2 or 4 hours (Chase/2h or Chase/4h) to monitor recycling of internalized antibody/ $\beta 1$ integrin to the surface, which was detected with a fluorescein isothiocyanate (FITC)-labeled secondary antibody. Quantification of total immunofluorescence intensity indicated that there was no significant difference in basal surface binding of clone 9EG7 (Fig. 2, A and B) or clone MB1.2 that recognizes $\beta 1$ integrin independently of conformation (fig. S3) between WT cells and those lacking CD13. However, whereas recycled 9EG7 was readily apparent at the surface by both 2 and 4 hours after chase in CD13⁺ cells, it was markedly lower in CD13-negative cells. Conversely, in permeabilized cells, the abundance of cytoplasmic 9EG7 was higher in CD13^{KO} MEFs when compared to WT cells (Fig. 2, A and B). These findings were confirmed by flow cytometric analysis of surface $\beta 1$ integrin (9EG7) expression under similar experimental conditions (Fig. 2C). Last, consistent with a role for CD13 in $\beta 1$ integrin recycling mechanisms, treatment of WT MEFs with the recycling inhibitor primaquine substantially reduced WT 9EG7-surface expression to that of CD13^{KO} MEFs (Fig. 2C).

Because a round of integrin recycling occurs over minutes, the relatively extended chase periods in these experiments likely reflect a composite effect of CD13 on both recycling and internalization. To investigate the effects of CD13 on the relative rates of internalization and recycling at earlier time points, we used a capture ELISA-based pulse-chase assay (Fig. 2, D and E), as described in (20). Total cell surface proteins were labeled with biotin, followed by internalization in label-free conditions. Cells were harvested over a period of 0 to 30 min, and the intracellular integrin pool was measured by ELISA and presented as a percentage of the initial surface-labeled $\beta 1$ integrin (Fig. 2D). Alternatively, to assess integrin recycling, surface-biotinylated proteins were given time to internalize followed by a chase period in complete medium for 30 min. The proportion of recycled integrin was calculated on the basis of the loss of internalized integrin in the cells after chase (Fig. 2E; see also Materials and Methods). Consistent with our immunofluorescence and flow cytometric analysis, loss of CD13 diminished 9EG7 recycling to the surface by 12 and 27% by 10 and 30 min of chase, respectively. To determine whether $\beta 1$ integrin trafficking was affected by the lack of its CD13 partner in human cells as well, we analyzed $\beta 1$ integrin recycling in our panel of transfected C33A human cell lines by immunofluorescence and flow cytometric analysis using the mAb to human $\beta 1$ integrin 12G10 (Fig. 3, A and B). Similar

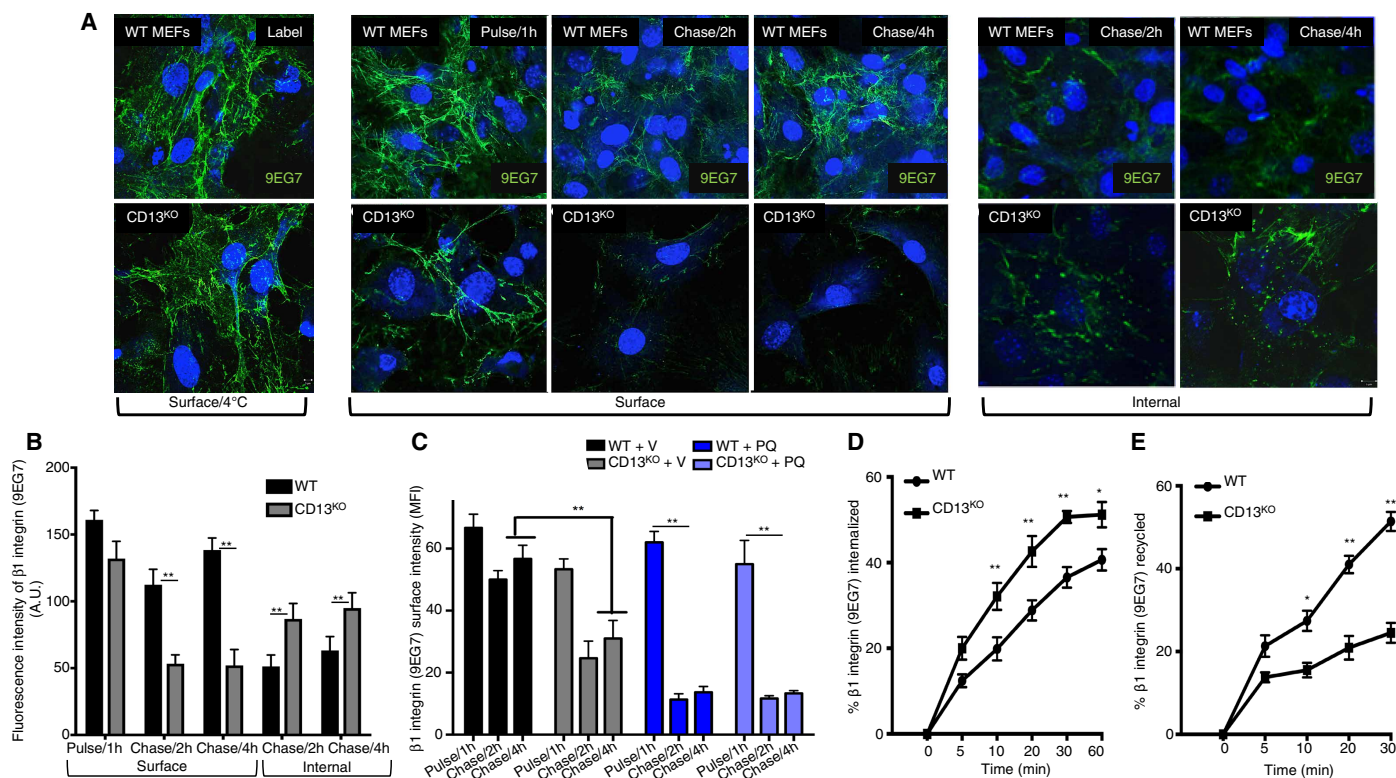


Fig. 2. Reduced $\beta 1$ integrin recycling in MEFs lacking CD13. (A to C) Recycling of surface $\beta 1$ integrin (green) was tracked in pulse-chase assays in WT and CD13^{KO} MEFs grown on FN. Cell surface $\beta 1$ integrin was tagged with unlabeled monoclonal antibody (mAb) clone 9EG7 for 30 min on ice, followed by incubation at 37°C (Pulse) for 1 hour to allow internalization. After pulse, cells were acid-stripped and washed to remove remaining surface antibody and chased for 2 or 4 hours in antibody-free medium (Chase/2h or Chase/4h). After chase, FITC-labeled secondary Ab was added to either fixed cells to detect recycled surface integrin or to permeabilized and fixed cells to detect both recycled and internalized 9EG7 by immunofluorescence analysis (A), quantification of fluorescence intensity of 9EG7 by Fiji software (B), and flow cytometry (C) in the presence of vehicle (V) or the recycling inhibitor primaquine (PQ; 1 μ M). Cells were counterstained with 4',6-diamidino-2-phenylindole (DAPI; blue). Scale bars, 5 μ m. (D and E) Biotin-labeled surface integrin was measured by capture enzyme-linked immunosorbent assay (ELISA) using 9EG7 mAb to determine % internalized 9EG7 (D) and % recycled 9EG7 (E) over time in WT and CD13^{KO} MEFs. Data are means \pm SD of three independent experiments. * P < 0.05 and ** P < 0.01 by two-tailed Student's *t* test. A.U., arbitrary units; MFI, mean fluorescence intensity.

to CD13^{KO} MEFs, β 1 integrin failed to recycle back to the plasma membrane in C33A-EV cells lacking CD13. Cells expressing the inactivatable phospho-tyrosine HCD13 mutant C33A-Y6F at an abundance equivalent to that of C33A-HCD13 were also recycling defective (Fig. 3, A to D), suggesting that active CD13 is necessary for proper β 1 integrin recycling to the cell surface. Flow cytometric analysis of our panel of cells treated with the recycling inhibitor primaquine showed reductions in C33A-HCD13 WT 12G10 surface abundance to that of the C33A-EV or C33A-Y6F mutant (Fig. 3C). Last, to confirm our studies in an additional loss-of-function model, we generated clones harboring a CRISPR-based deletion of CD13 in the human KS endothelial model cell line KS1767. We have previously shown that these express high amounts of CD13 comparable to primary human umbilical vein endothelial cells and that CD13 is physiologically relevant in these cells (19, 21, 22). Flow cytometric analysis indicated a total loss of CD13 expression in the CD13 CRISPR KS clones compared to control clones containing scrambled guide RNAs (fig. S4A). Similar to MEFs and epithelial cells, lack of CD13 expression led to markedly diminished cell-ECM adhesion, migration, and recycling in two independent CD13 CRISPR KS clones compared to controls (fig. S4, B to E). Therefore, our data together indicate that CD13 regulates β 1 integrin recycling in both humans and mice, in

cells of distinct origin and in loss-of-function (endogenously CD13⁺ primary murine WT and CD13^{KO} fibroblasts and WT and CD13^{KO} CRISPR-engineered KS endothelial cells) and gain-of-function (C33A stably transfected cancer epithelial cell lines) studies.

CD13 regulates endocytic trafficking of β 1 integrin to Rab11⁺ recycling endosomes

Recycled β 1 integrin generally follows a path from Rab5⁺ early endosomes to Rab11⁺ perinuclear recycling endosomes and is ultimately recycled back to the plasma membrane (8, 23). To determine whether the lack of CD13 affects this well-characterized pathway, we tracked the endocytic fate of internalized β 1 integrin in the presence or absence of CD13 by immunofluorescence (Fig. 4, A and B). Analysis of β 1 integrin trafficking in WT or CD13^{KO} MEFs grown on FN using mAb 9EG7 illustrated that, regardless of CD13 expression, β 1 integrin initially internalized into the Rab5⁺ early endosomes within 5 min (24). However, as trafficking proceeds, β 1 integrin accumulates in Rab11⁺ recycling endosomes after 60 min in WT cells but appears to be redirected to Rab7⁺ lysosomes in the absence of CD13 (Fig. 4A). We confirmed these changes in localization by determining the linear correlation between β 1 integrin and the various endosomal markers by Pearson's correlation coefficient (r ; Fig. 4B).

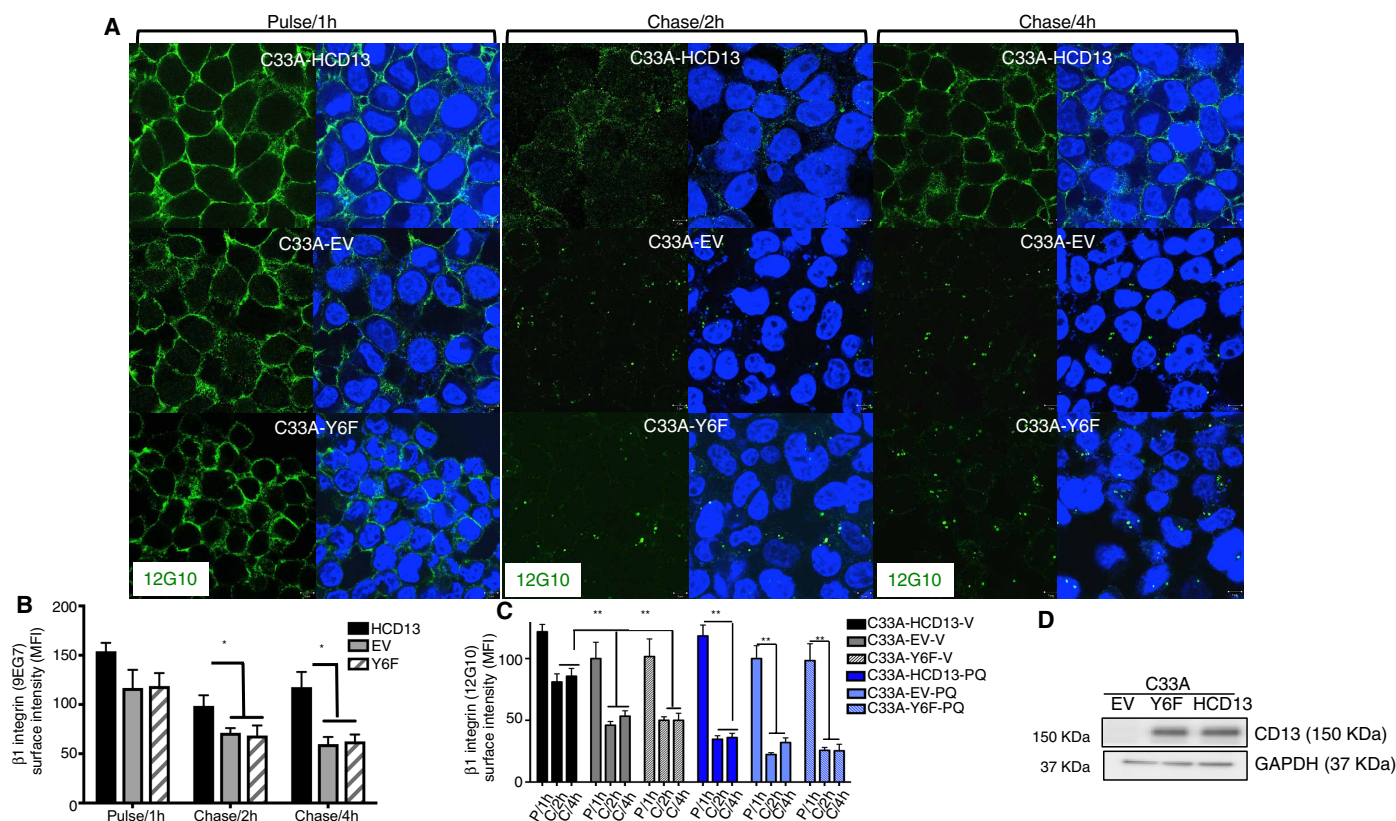


Fig. 3. β 1 integrin recycle to the surface in epithelial cells expressing CD13 but not in the absence of CD13 or cells expressing CD13 phospho-tyrosine mutant.

(A) In a pulse-chase assay, human β 1 integrin was labeled with Ab clone 12G10, and expression of β 1 integrin (green) was tracked in antibody-pulsed cells for 1 hour (P/1h) followed by chase in antibody-free medium for 2 or 4 hours (C/2h or C/4h) by immunofluorescence analysis. Cells were counterstained with DAPI (blue), fixed, and imaged by confocal microscopy. Scale bars, 5 μ m. (B) Quantification of fluorescence intensity of 12G10 staining shown in (A) using Fiji software. (C) β 1 integrin receptor surface recycling was measured in a pulse-chase assay with flow cytometric analysis of human β 1 integrin Ab clone 12G10 in C33A cells expressing EV, HCD13, or Y6F in the presence or absence of recycling inhibitor primaquine (1 μ M). (D) Equivalent level of CD13 expression in C33A expressing phospho-tyrosine mutant Y6F compared to HCD13 indicated by Western blot analysis. Images (A) are representative and data (B to D) are means \pm SD of three independent experiments. * P < 0.05 and ** P < 0.01 by two-tailed Student's t test.

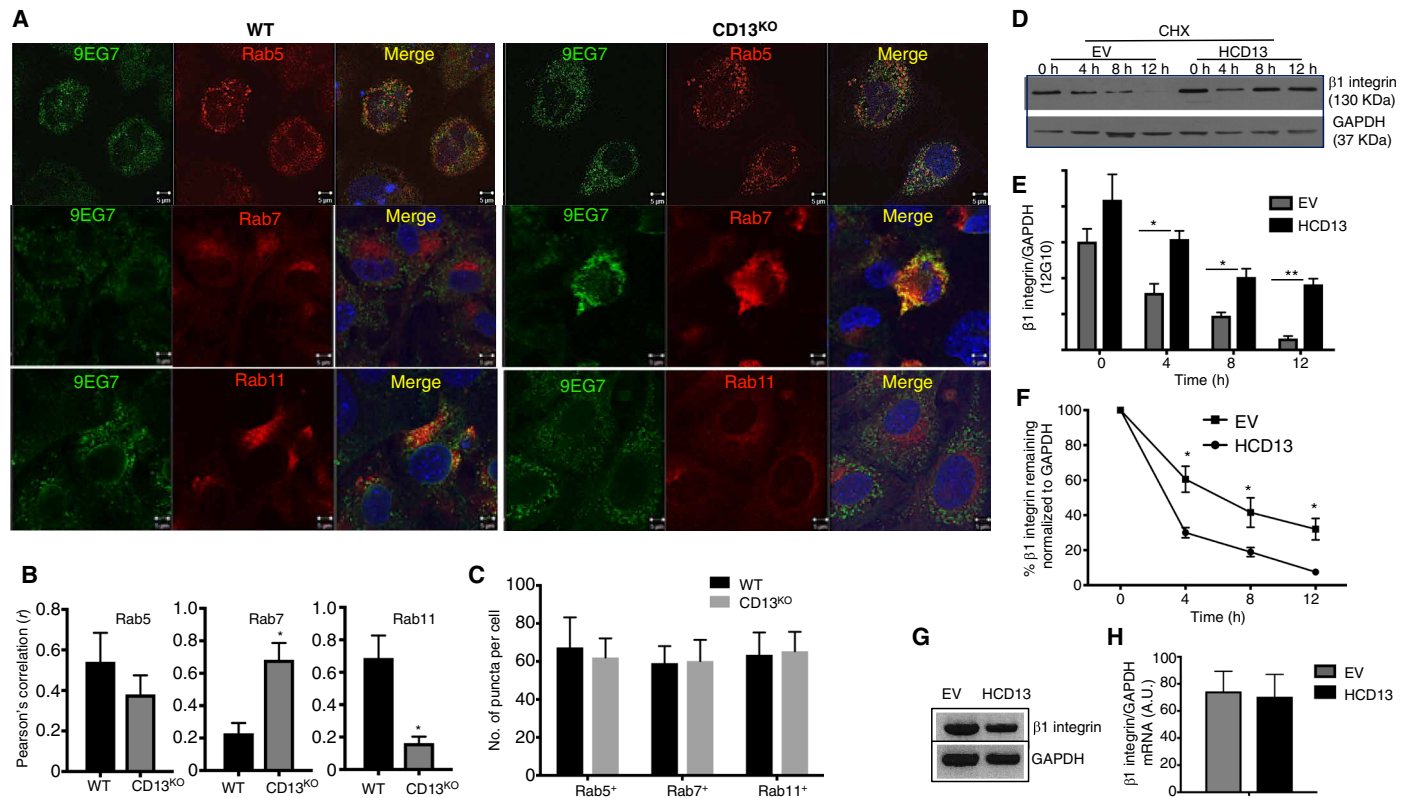


Fig. 4. β 1 integrin is directed to the lysosome for degradation in the CD13 deficient cells. (A) Cells were grown on FN for 0 to 60 min, and cells were fixed and stained for β 1 integrin (9EG7; green) and one of three endosomal markers (red): Rab5 (early endosomal marker), Rab7 (late endosomal/lysosomal marker), and Rab11 (recycling endosomal marker). Cells were counterstained with DAPI (blue). Scale bars, 5 μ m. Blots are representative of three independent experiments. (B) Images represented in (A) were quantified by MetaMorph software, and correlation coefficient (r) values of β 1 integrin (9EG7) with endosomal markers determined by Pearson's analysis are shown. $*P < 0.05$ by two-tailed Student's t test. (C) Quantification of Rab5⁺, Rab7⁺, or Rab11⁺ puncta per cell for in WT and CD13^{KO} MEFs. All cells in a field were counted, and five fields were counted for each genotype. (D) C33A cells expressing EV and HCD13 were treated with cycloheximide (CHX; 100 μ g/ml) to inhibit new protein synthesis for the indicated time. Cell lysates were analyzed by immunoblotting for β 1 integrin using the mAb 12G10. Glyceraldehyde-3-phosphate dehydrogenase (GAPDH) served as a loading control. Blots are representative of three independent experiments. (E and F) Quantification of immunoblot analysis represented in (D) by ImageJ Pro as a ratio of 12G10 to GAPDH or 12G10 normalized to time = 0 hours. Data are means \pm SD of three independent experiments. (G and H) Total RNA was extracted from C33A cells expressing EV or HCD13 treated with cycloheximide for the indicated time, and the abundance of *ITGB1* (β 1 integrin) and *GAPDH* mRNA was determined by Real-time PCR run on ethidium bromide-stained gels. Gels were analyzed by ImageJ Pro, and the ratio was plotted. Data in (B), (C), (E), (F), and (H) are means \pm SD of three independent experiments. $*P < 0.05$ and $**P < 0.01$ by two-tailed Student's t test.

In addition, the number of Rab5, Rab7, and Rab11 puncta per cell was equivalent between genotypes, arguing that a lack of CD13 does not grossly affect endosome number or formation (Fig. 4C), although it may affect endosomal distribution patterns [Fig. 4A: Rab11, WT versus KO (knockout)].

To determine the eventual fate of β 1 integrin in the absence of CD13, we pretreated epithelial cells with cycloheximide to inhibit new protein synthesis. Immunoblot analysis indicated that β 1 integrin abundance decreased over time and was diminished below detection by 12 hours in culture in the C33A-EV cells, unlike in WT cells (Fig. 4, D to F), indicating that CD13 participates in directing endosomal β 1 integrin to the recycling pathway and thus controls cell surface expression. Real-time polymerase chain reaction (PCR) analysis confirmed that decreased β 1 integrin protein in CD13^{KO} cells is not due to effects on gene transcription, because we detected equivalent amounts of β 1 integrin transcripts in both genotypes, suggesting that the loss of β 1 integrin protein in cells lacking CD13 is a posttranscriptional event (Fig. 4, G and H), consistent with enhanced lysosomal degradation in the absence of CD13.

Active CD13 forms a complex with ARF6-GTP and IQGAP1

We have previously demonstrated that coimmunoprecipitation of CD13 with IQGAP1, an effector of the Rho family of small GTPases and a fundamental regulator of cell migration (25), is necessary to promote CD13-mediated cell-cell adhesion (15). IQGAP1 is a multifunctional scaffolding protein that recruits, assembles, and activates small GTPases and their effectors to integrate cellular functions (26, 27). Relevant to potential mechanisms by which CD13 affects β 1 integrin recycling, IQGAP1 also interacts with and activates the small GTPase ARF6, which is required for proper β 1 integrin trafficking and recycling (7, 8, 27–30). To assess the possibility that CD13 affects β 1 integrin recycling by an IQGAP1-ARF6-mediated mechanism, we immunoprecipitated lysates of our panel of epithelial cell lines expressing EV, WT, or Y6F-HCD13 with anti-HCD13 mAb 452 or isotype control. Analysis of the complex showed that it contained abundant IQGAP1 by Western blot and detectable amounts of active ARF6 [as assessed by binding to the protein-binding domain (PBD) of the ARF6 effector protein GGA3] only in those cells expressing WT CD13 but not the EV or the Y6F mutant (Fig. 5A). Similarly,

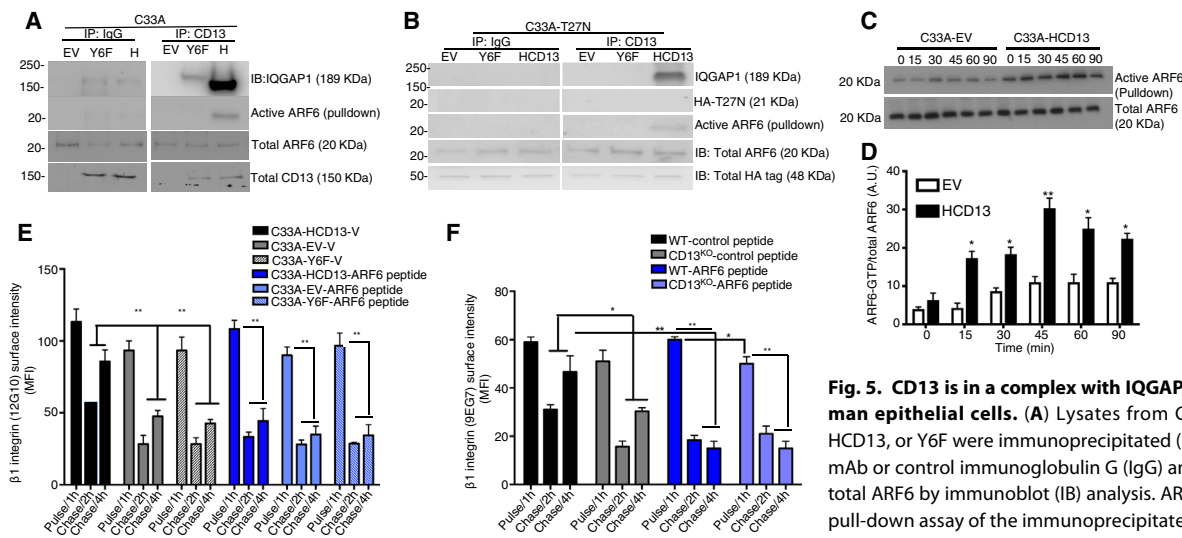


Fig. 5. CD13 is in a complex with IQGAP1 and active ARF6 in human epithelial cells.

(A) Lysates from C33A cells expressing EV, HCD13, or Y6F were immunoprecipitated (IP) with biotinylated CD13 mAb or control immunoglobulin G (IgG) and probed for IQGAP1 and total ARF6 by immunoblot (IB) analysis. ARF6-GTP was detected by a pull-down assay of the immunoprecipitates using beads conjugated to the PBD of GGA3 for 1 hour at 4°C. (B) Lysates from T27N ARF6 C33A cells expressing EV, HCD13, or Y6F were immunoprecipitated (IP) with biotinylated CD13 mAb or control immunoglobulin G (IgG) and probed for IQGAP1 and total ARF6 by immunoblot (IB) analysis. ARF6-GTP was detected by a pull-down assay of the immunoprecipitates using beads conjugated to the PBD of GGA3 for 1 hour at 4°C. (C and D) ARF6 activity was measured in C33A cells expressing EV or HCD13 after cell-ECM adhesion over the indicated time. Using ARF6 PBD of the effector protein GGA3-conjugated beads, which specifically binds the GTP-bound form of ARF6, the subsequent pull-down of ARF6-GTP was quantified by immunoblot analysis using the ARF6-specific antibody. Blots (C) are representative of and quantified data (D) are means \pm SD of three independent experiments. (E and F) β 1 integrin receptor recycling was measured in a pulse-chase assay with β 1 integrin Ab clone 12G10 [for C33A cells; (E)] or 9EG7 [for MEFs; (F)] in the presence of N-myristoylated ARF6 inhibitor peptide. Serum-starved cells were treated with β 1 integrin Ab at 4°C for 30 min, pulsed for 1 hour to induce internalization, acid-stripped, washed, treated with myr-ARF6 peptide (10 μ M) for 30 min, and allowed to recycle at 37°C for 2 to 4 hours. Paraformaldehyde-fixed cells were stained with fluorescently conjugated secondary Ab, and MFI of surface β 1 integrin was analyzed by flow cytometry. Data are means \pm SD of three independent experiments. * P < 0.05 and ** P < 0.01 by two-tailed Student's *t* test.

dominant-negative mutant cells expressing EV, HCD13, or Y6F were immunoprecipitated with biotinylated CD13 mAb or control IgG and probed for IQGAP1, ARF6, or HA tag by immunoblot analysis. Active ARF6 was detected by pull-down with GGA3-conjugated beads from the immunoprecipitates. (C and D) ARF6 activity was measured in C33A cells expressing EV or HCD13 after cell-ECM adhesion over the indicated time. Using ARF6 PBD of the effector protein GGA3-conjugated beads, which specifically binds the GTP-bound form of ARF6, the subsequent pull-down of ARF6-GTP was quantified by immunoblot analysis using the ARF6-specific antibody. Blots (C) are representative of and quantified data (D) are means \pm SD of three independent experiments. (E and F) β 1 integrin receptor recycling was measured in a pulse-chase assay with β 1 integrin Ab clone 12G10 [for C33A cells; (E)] or 9EG7 [for MEFs; (F)] in the presence of N-myristoylated ARF6 inhibitor peptide. Serum-starved cells were treated with β 1 integrin Ab at 4°C for 30 min, pulsed for 1 hour to induce internalization, acid-stripped, washed, treated with myr-ARF6 peptide (10 μ M) for 30 min, and allowed to recycle at 37°C for 2 to 4 hours. Paraformaldehyde-fixed cells were stained with fluorescently conjugated secondary Ab, and MFI of surface β 1 integrin was analyzed by flow cytometry. Data are means \pm SD of three independent experiments. * P < 0.05 and ** P < 0.01 by two-tailed Student's *t* test.

expression of the hemagglutinin (HA)-tagged, inactive, dominant-negative ARF6 mutant ARF6-T27N-HA in our panel of cell lines illustrated that, although equivalent amounts of HA-tagged protein are present in the cell lysate, inactive ARF6-HA does not associate with WT CD13 (Fig. 5B). Because only the endogenous WT ARF6 can be activated, whereas the mutant protein sequesters ARF6-GEFs but remains completely inactive (31), this result implies that CD13 only interacts with the active GTP-bound form of ARF6. The low abundance of ARF6-T27N-HA expressed in these lines enables sufficient residual, unbound ARF6 GEFs to activate endogenous ARF6. In addition, in a cell-ECM adhesion assay, monitoring ARF6 activation over time by its ability to bind GGA3 illustrated that ARF6 activation is consistently and persistently reduced in the absence of CD13 (Fig. 5, C and D). Furthermore, specifically blocking ARF6 activity with the N-terminal effector domain inhibitory peptide (32, 33) in WT cells recapitulates the loss of β 1 integrin cell surface expression in CD13^{KO}- or CD13-Y6F-containing cells by flow cytometry, further supporting a direct regulation of ARF6 by CD13 (Fig. 5, E and F). Therefore, in WT cells, CD13, ARF6, and IQGAP1 are present in a complex that depends on both CD13 phosphorylation and activated ARF6. In addition, CD13 promotes optimal ARF6 activation and β 1 integrin surface expression.

CD13 recruits IQGAP1/ARF6 complex to the leading edge in migration

In motile cells, IQGAP1 is recruited to the migrating front where it cross-links actin filaments at the plasma membrane to enable directional migration (27, 28, 34). Analysis of our panel of epithelial cell lines in *in vitro* wound healing assays showed that IQGAP1 and F-actin are localized to the leading edge of migrating cells at higher levels in the presence of WT CD13 (Fig. 6, A to C), suggesting that active,

phospho-CD13 enhances IQGAP1 recruitment to the plasma membrane during migration (31). In agreement with this notion, CD13 also accumulates at the leading front, where it is coincident with IQGAP1 expression (Fig. 6, A to C). In addition, the number of cells with F-actin, CD13, and IQGAP1 localized at the leading front was substantially lower in cells containing the EV or Y6F mutant constructs compared to their WT counterparts (Fig. 6D). Western blot analysis of fractionated cells confirmed that membrane-resident IQGAP1 abundance increased in the presence of WT CD13 when compared to control or mutant cells (Fig. 7, A and B). In addition, active ARF6-GTP was found only in the membrane fraction in cells expressing WT but not mutant CD13 (compared to E-cadherin membrane expression), whereas total (active and inactive) membrane-localized ARF6 abundance remained unchanged (Fig. 7, A and B). Last, hyperactivation of heterotrimeric GTP-binding proteins (including ARF6) (35) with aluminum fluoride (AlF) increased the abundance of active ARF6 at the membrane, but again only in the presence of WT CD13 (Fig. 7, A and B, and fig. S5), suggesting that localization of active ARF6 at the membrane is CD13 dependent or that interaction with CD13 is important to maintain ARF6 activation.

Membrane localization of the ARF6-GEF EFA6 requires WT CD13

The cyclic activation of ARF6 and other GTPases is regulated by activating GEFs that enable the exchange of protein-bound guanine diphosphate (GDP) to GTP and GTPases that terminate signaling by hydrolyzing GTP to GDP. To determine the mechanism by which CD13 regulates ARF6 activation, we focused on two ARF6-activating GEFs, EFA6 and ARNO, which have been shown to regulate β 1 integrin traffic and transport (36–38). These GEFs are membrane-tethered, but are not integral membrane proteins, suggesting that auxiliary

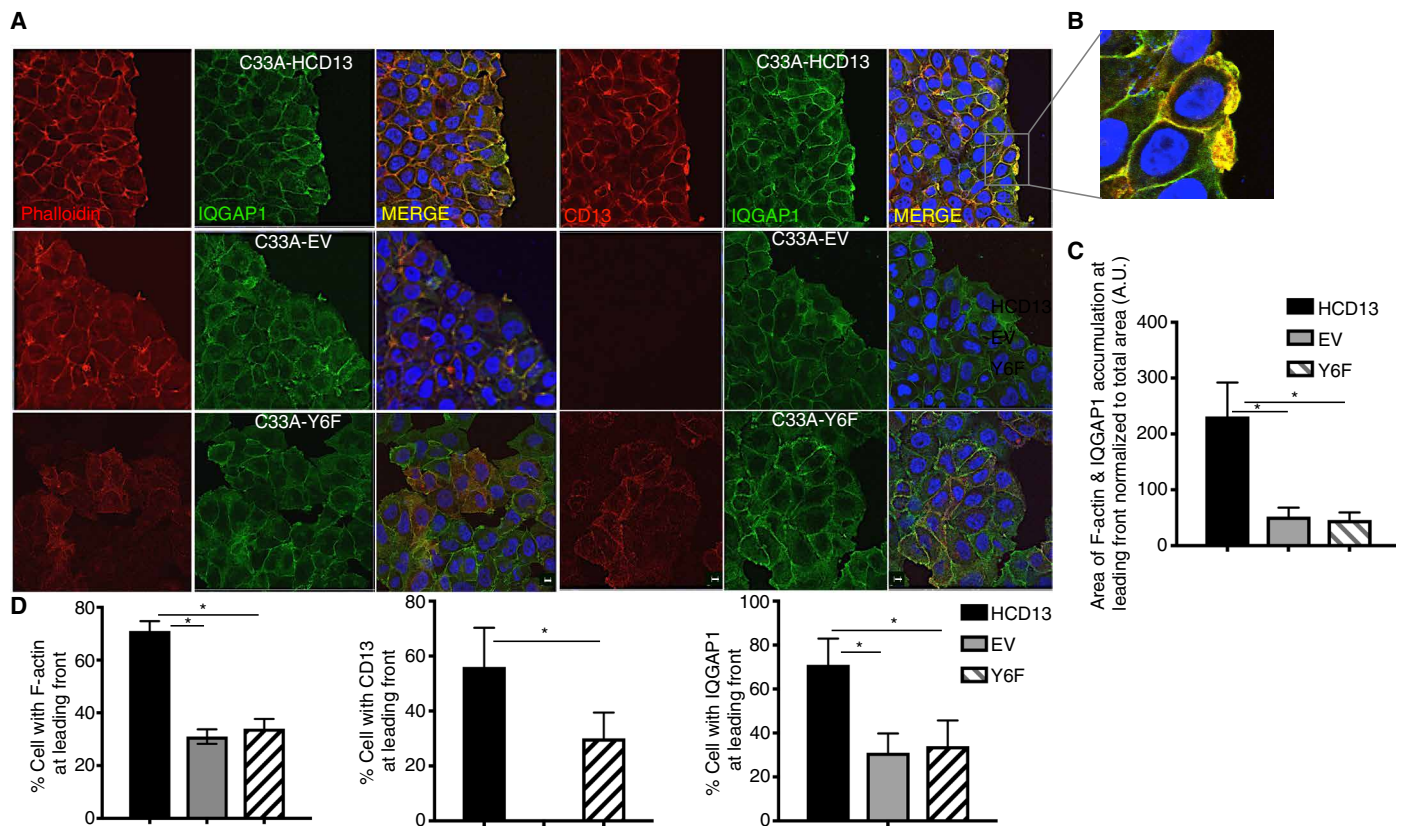


Fig. 6. CD13 recruits IQGAP1 at the leading edge in directional cell migration. (A and B) In a scratch assay, after injury on the monolayer by creating a scratch, C33A cells expressing HCD13 were allowed to migrate to the wound and fixed with 4% paraformaldehyde at the 6-hour time point. Cells were stained with phalloidin (red; left rows) or CD13 (red; right rows) and IQGAP1 (green) and imaged using confocal microscopy; magnified inset of CD13/IQGAP1-stained C33A-HCD13 cells is shown (B). Scale bars, 5 μ m. DAPI (blue). (C) Quantification of the area of F-actin and IQGAP1 accumulation at the migrating front of the cell, represented in (A), normalized to total cell area by Fiji software. Five fields were counted for each genotype, and all cells in each field were measured. (D) Percentages of F-actin⁺, CD13⁺, and IQGAP1⁺ cells from (A) at the leading front were measured in each of five fields for each genotype. Data are means \pm SD of three independent experiments. * P < 0.05 by two-tailed Student's t test.

transmembrane proteins may guide the GEFs to the plasma membrane to activate ARF6 (39, 40). We addressed this possibility by coimmunoprecipitation analysis of lysates from C33A cells with CD13 mAb 452 or control IgG. Western blot analysis indicated that EFA6 but not ARNO was present in the immunoprecipitated complex in cells expressing HCD13 but not EV or Y6F (Fig. 8, A and B), consistent with CD13 acting as an EFA6 membrane tether. In support of this notion, we found that EFA6 was localized at the leading edge of migrating cells expressing HCD13, where it coincided with CD13 (Fig. 8, C and D), by immunofluorescence and confocal image analysis. Quantification showed that the number of EFA6⁺ puncta at the leading edge was markedly higher in cells expressing HCD13 compared to that in cells expressing EV or Y6F, thereby establishing that EFA6 is likely the GEF for ARF6 in this context. Together, we conclude that CD13 must be present in a complex containing the scaffolding protein IQGAP1, the ARF6 GEF, EFA6, active ARF6, and β 1 integrin at the plasma membrane for β 1 integrin trafficking and cell migration to proceed normally. In the absence of CD13, EFA6 is no longer membrane localized, ARF6 is not activated, and β 1 integrin trafficking is dysregulated and is eventually degraded, leading to reduced cell migration (Fig. 9). Therefore, this study describes a previously unknown role for CD13 as a membrane tether and expands its functional contribution to the control of fundamental cellular processes such as GTPase activation, receptor recycling, cell-ECM interactions, adhesion, and migration.

DISCUSSION

By establishing communication with the external matrix, integrins trigger complex internal mechanisms by dictating membrane and cytoskeletal interactions that are critical to regulate cell shape and coordinated movement. Consequently, the various endocytic and recycling routes that control integrin trafficking assume an essential role as regulators of the cell surface integrin profile, stability, and, ultimately, cell migration (28). These routes of integrin internalization and recovery are acutely tied to numerous components of signal transduction pathways, various molecular switches, and the cytoskeletal machinery at different points along the route, regulating internalization, sorting, trafficking, and recycling/degradation. As our appreciation of the widespread biological impact of integrin trafficking expands, the number of proteins of all types identified as contributors and mediators of these pathways is escalating, revealing a tremendous complexity in these systems and highlighting that much work remains to be done. In the current study, we identify the transmembrane protein CD13 as a previously unknown mediator of β 1 integrin recycling that is located in a complex enriched in IQGAP1, EFA6, and active ARF6 proteins. Mechanistically, we show that WT but not mutant CD13 recruits IQGAP1 and EFA6 to the leading edge, allowing ARF6 activation that is necessary for ARF6-mediated β 1 integrin expression on the cell surface, whereas in cells lacking CD13, β 1 integrin accumulates in late endosomes and is eventually degraded.

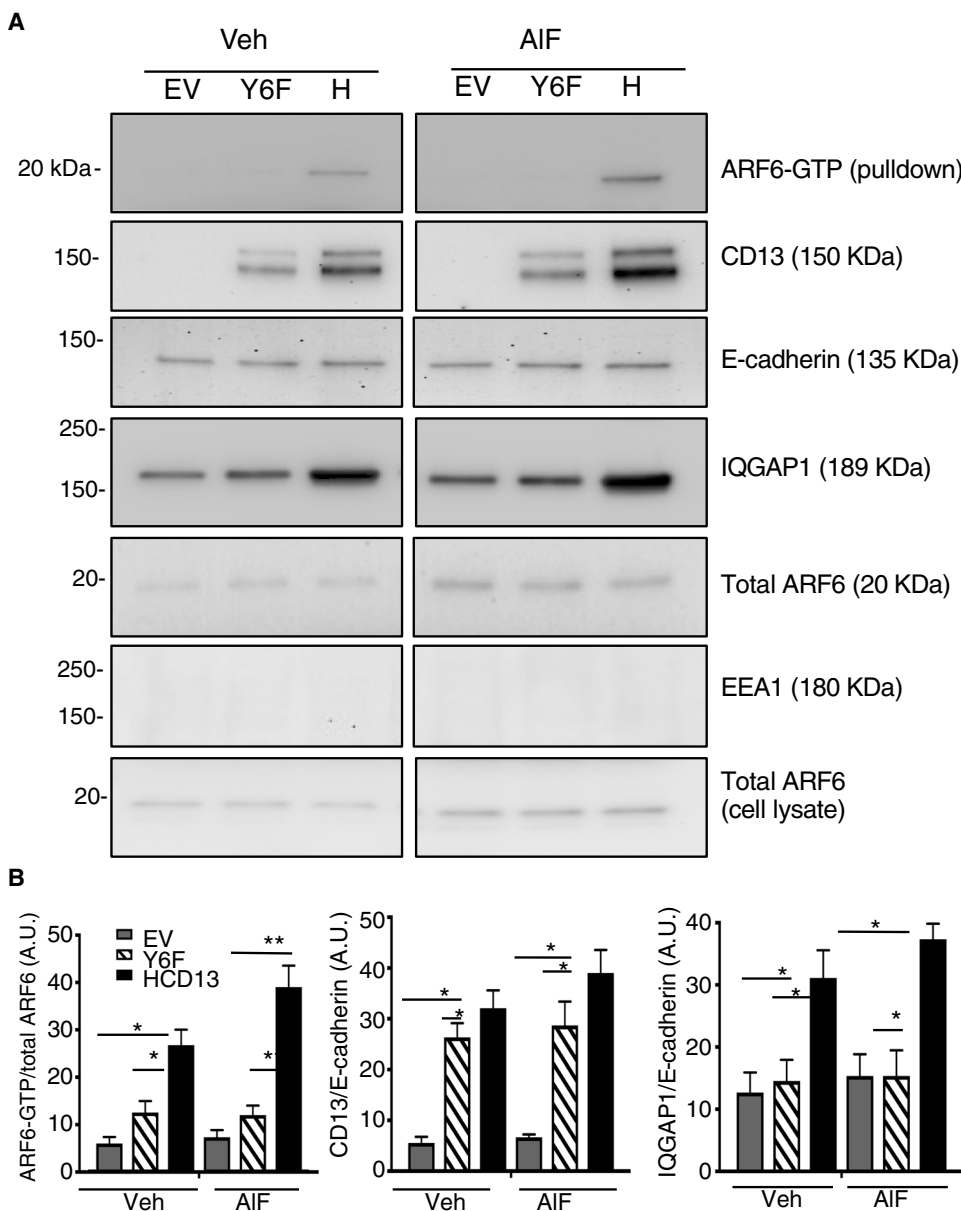


Fig. 7. CD13 phosphorylation is necessary for maintenance of ARF6 activation. (A) C33A cells expressing EV, HCD13, or Y6F were treated with vehicle (Veh) or AIF (50 μ M) for 30 min, and membrane fractions were purified from total cell lysates. Active ARF6-GTP in the fractions was measured by pull-down assay and normalized to total ARF6. Validation of the membrane fraction was verified by expression of plasma membrane marker E-cadherin. (B) Plots depict quantification of immunoblot analysis of ARF6-GTP, CD13, and IQGAP1 normalized to E-cadherin in the plasma membrane. Data are means \pm SD of three independent experiments. * P < 0.05 and ** P < 0.01 by two-tailed Student's t test.

Internalization of integrins occurs by various mechanisms, including both clathrin-dependent and clathrin-independent endocytosis (41, 42). Initially, most internalized receptors traffic to the early endosomes, where sorting signals are interpreted to dictate recycling to the surface or degradation in late endosomes/lysosomes. Relevant to our study, it is thought that internalized integrins traffic to lysosomes by default and thus are degraded unless specifically recruited into recycling routes by interacting with trafficking regulators (28). For example, proteins such as the Arp2/3 activator WASH (43), SNX17 (44), or CLIC3 (41, 42) can

bind to integrins and divert their trafficking away from lysosomes, maintaining levels of surface integrin. It is possible that CD13 also functions as such a regulator of β 1 integrin endocytic recycling, and thus, β 1 integrin is degraded in its absence. Alternatively, Rab11 staining appears to be more diffuse in the CD13^{KO} cells, perhaps suggesting a role for CD13 in the dispersal of the recycling endosome to affect recycling. Although our study adds to our limited knowledge of the molecules and mechanisms regulating endosomal distribution and integrin endocytic fate, the relative specificity of these for individual integrin pairs is still unknown. The tissue-specific expression and signaling of distinct integrin heterodimers would suggest that specific trafficking mechanisms and regulators exist (3). Therefore, similar studies identifying additional regulatory proteins will be important to allow us to decipher whether trafficking regulators such as CD13 are responsible for trafficking patterns of specific integrin pairs and/or their signaling pathways.

Alternatively, integrin-ECM interactions at the plasma membrane trigger notable changes in intracellular cytoskeletal dynamics that affect trafficking and, consequently, integrin activity and function. The scaffolding protein IQGAP1 interacts with nearly a hundred proteins to assemble complexes with defined cell functions and so translates incoming receptor-mediated signals into operational nodes to relay functional outputs [reviewed in (45, 46)]. IQGAP1 has been implicated in control of cytoskeletal organization by directly interacting with and organizing F-actin and other adaptor proteins, regulation of intracellular trafficking routes by activation of the small GTPase ARF6 (27), and directing cell-ECM interactions by modulating β 1 integrin recycling (8, 30).

We have previously reported that CD13 and IQGAP1 interact constitutively to promote inflammatory myeloid-endothelial adhesion in a non-ECM adherent monocytic cell line U937 (15), whereas in this study, we find that CD13 must be phosphorylated at Tyr⁶ to interact with and enhance IQGAP1 localization to the leading edge in migrating epithelial cells. This discrepancy could be due to differences in cell types (adherent versus nonadherent) or distinct requirements for cell-cell versus cell-ECM interactions. Last, another protein, the 4.1R protein, Ezrin, Radixin, Moesin-containing 4.1R, has been demonstrated to directly bind IQGAP1 and recruit it to the plasma membrane, allowing subsequent engagement of

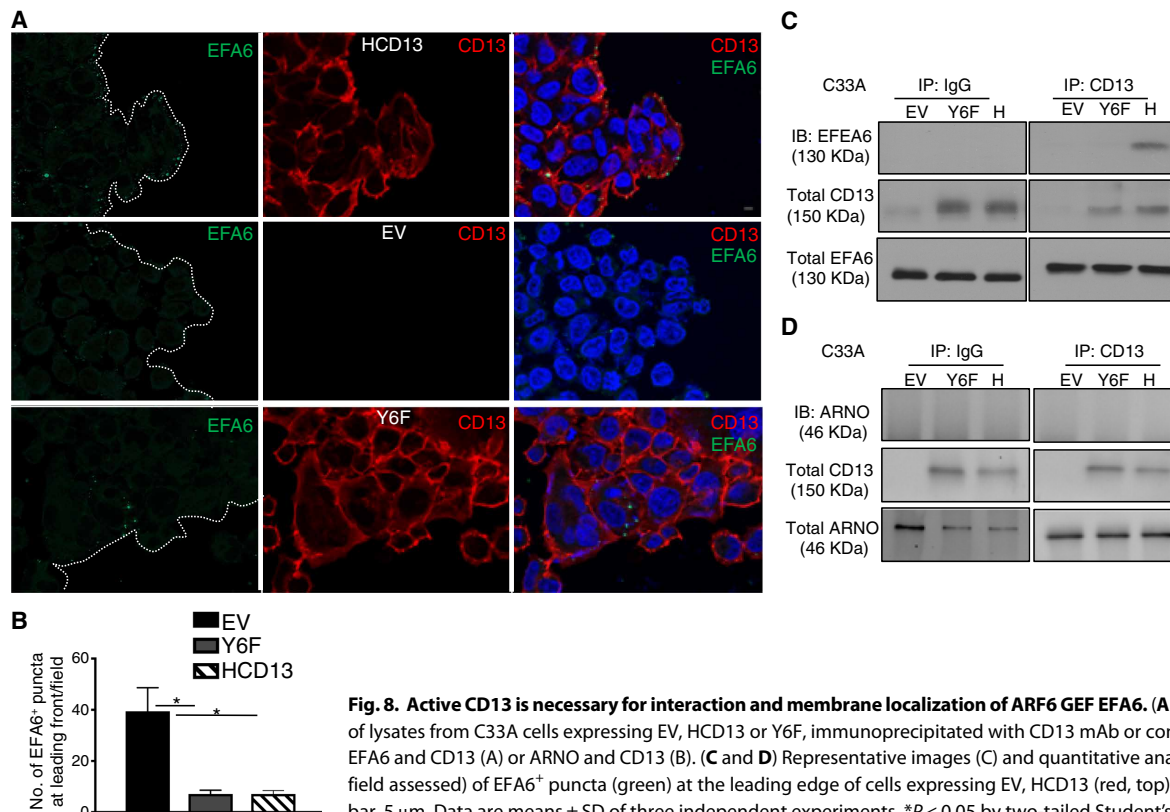


Fig. 8. Active CD13 is necessary for interaction and membrane localization of ARF6 GEF EFA6. (A and B) Immunofluorescence analysis of lysates from C33A cells expressing EV, HCD13 or Y6F, immunoprecipitated with CD13 mAb or control IgG and probed (IB) for EFA6 and CD13 (A) or ARNO and CD13 (B). (C and D) Representative images (C) and quantitative analysis (D) of the number (per field assessed) of EFA6⁺ puncta (green) at the leading edge of cells expressing EV, HCD13 (red, top), or Y6F (red, bottom). Scale bar, 5 μ m. Data are means \pm SD of three independent experiments. * $P < 0.05$ by two-tailed Student's *t* test.

downstream IQGAP1-binding proteins to facilitate cell migration. However, the mechanism of 4.1R localization at the leading edge is not known but is postulated to cotraffic either with polarized membrane lipids such as phosphatidylinositol 4,5-bisphosphate [PI(4,5)P₂] or with redistributing transmembrane receptors (34). In contrast, CD13 itself actively redistributes to polarized areas in numerous cell types where it accumulates at points of cell-cell contact (14, 47), areas enriched in lamellipodia and filopodia (14, 19), sites of phagocytosis (48, 49), at the apical membrane in polarized renal and intestinal epithelial cells (50, 51), endothelial cells (52) and at cell-ECM contacts (current study), suggesting that, in some cellular processes, CD13 serves to ensure that IQGAP1 is properly positioned to perform its functions. Thus, it may be expected that CD13 participates in a number of functions also mediated by IQGAP1, such as phagocytosis (53), angiogenesis (54), cell motility (55), filopodia formation (56), and endocytosis (57). Further investigation into this possibility is underway.

The precise coordination of membrane and cytoskeletal dynamics and receptor trafficking required for the spatiotemporal regulation of integrin traffic is predominantly regulated by the Ras superfamily of small GTPases (Rho, Rab, and ARF families) and their effectors. In particular, the smallest family, the ARFs, tightly regulates membrane dynamics, and ARF6 has a critical role in both integrin internalization (58) and recycling mediated by IQGAP1 (8, 29, 30). GTPase activity is regulated by specific GEFs and GAPs, and we have demonstrated that, similar to β 1 integrin (8) and IQGAP1 (27), CD13 only interacts with the active GTP-bound form of ARF6. Furthermore, the membrane localization of both IQGAP1 and the ARF6-GEF, EFA6, is lost in the absence of CD13. Recent studies have shown

that the majority of endogenous EFA6 is membrane associated, as are its GEF-defective mutants, but is not itself an integral membrane protein. However, catalytically active constructs that contain mutations disrupting either of two domains necessary for EFA6 membrane localization, the PI(4,5)P₂-binding pleckstrin homology (PH) and the coiled-coil (CC) domains, are less active and are unable to recruit ARF6 to the plasma membrane. These observations confirm that EFA6 must be membrane-tethered to activate ARF6, raising the possibility that auxiliary transmembrane proteins such as CD13 may be required to guide or hold EFA6 at the plasma membrane (39, 40). Further studies confirmed that the PH and CC domains are required for membrane tethering and demonstrated that the CC domain associates with actin by binding the actin-binding protein α -actinin (59, 60). We have previously shown that both α -actinin and IQGAP1 are physically associated with CD13 in myeloid cells (15), suggesting that CD13 complexes with EFA6 by interaction with α -actinin. Therefore, CD13 recruits and tethers the complex containing IQGAP1, α -actinin, EFA6, and ARF6 at the plasma membrane, thus correctly positioning EFA6 to enable activation of ARF6 and regulate endosomal membrane recycling. This model is consistent with studies illustrating that recycling endosomes require EFA6 activation of ARF6 to allow fusion with the plasma membrane and promote β 1 integrin surface expression (39, 40). In this light, the proteins such as CD13 that position ARF6 and members of other families of small GTP-binding proteins and their regulatory GEFs and GAPs at specific locations become critical regulators of cell function. Similarly, as the importance of communication between ARF proteins and other small GTPases in the regulation of intracellular processes is rapidly emerging, identification

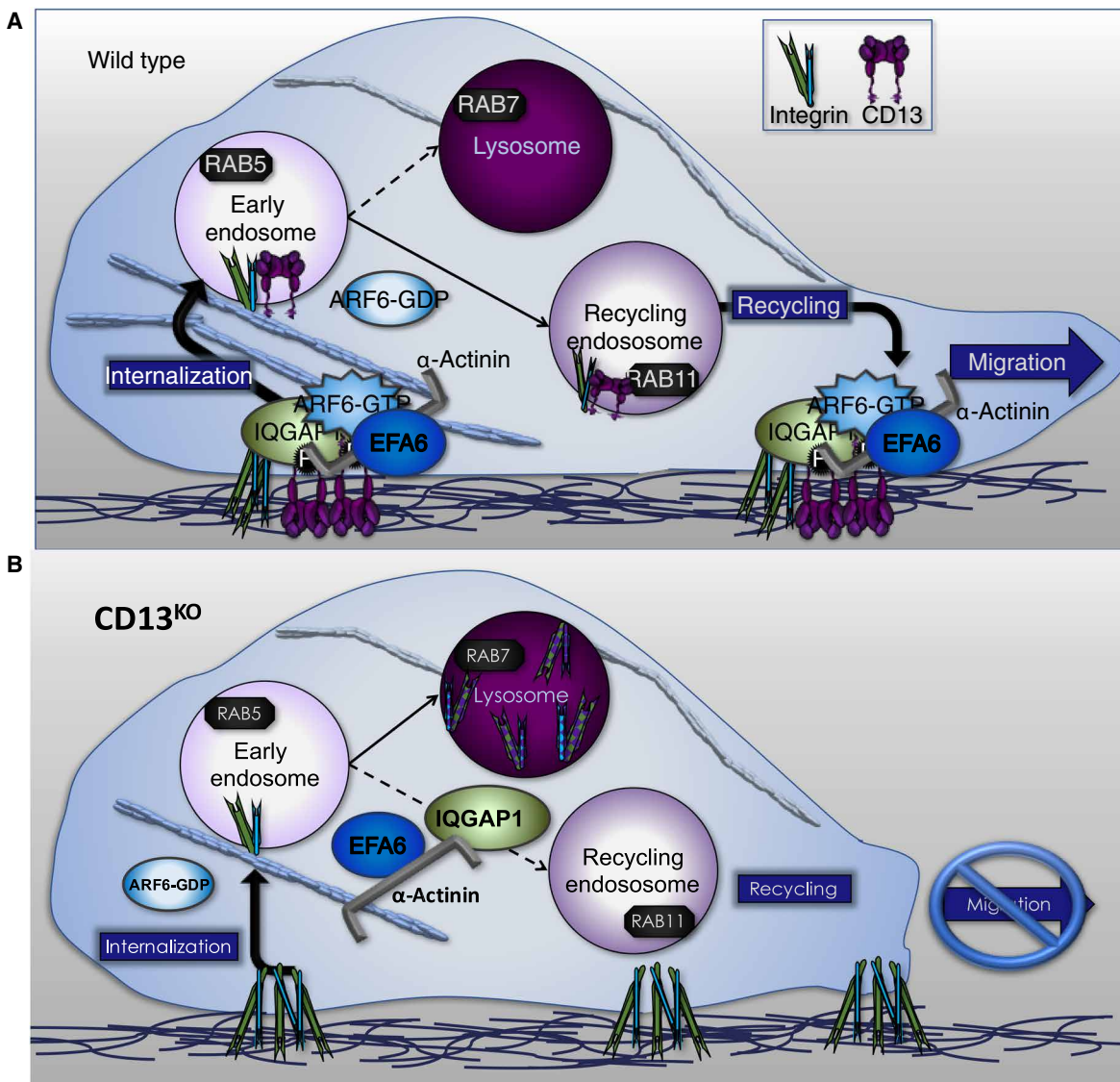


Fig. 9. Schematic of proposed mechanism. (A) In WT cells, phospho-CD13 and $\beta 1$ integrin internalize into early endosomes, sort to recycling endosomes, and return to the cell membrane, enabling cell-ECM adhesion and migration. (B) However, in cells lacking CD13 or expressing an inactive CD13 mutant, whereas $\beta 1$ integrin internalizes into early endosomes, it aberrantly traffics to Rab7⁺ lysosomes and is ultimately degraded. Mechanistically, CD13 must be present in a complex containing the scaffolding protein IQGAP1, active ARF6, its GEF EFA6, and $\beta 1$ integrin at the plasma membrane to allow proper $\beta 1$ integrin recycling and cell migration to proceed. In the absence of CD13, no active ARF6 is detected in the plasma membrane, and IQGAP1 is not recruited to the migrating front, thereby diminishing cell adhesion, spreading, and migration.

of novel interacting proteins and the interactions that they orchestrate will help clarify the complex cross-talk between signaling pathways mediated by multiple GTPases.

Our study strongly supports a role for CD13 in cell-ECM adhesion mediated by regulation of integrins that are fundamental components of numerous developmental, homeostatic, and disease processes, expanding the potential for CD13's participation in additional physiological processes. Although we have demonstrated here that CD13 controls integrin recycling, whether CD13 participates in other activities such as cell-ECM detachment and focal adhesion turnover is currently unknown. Similarly, endosomal delivery and turnover of transmembrane proteins is central to the homeostasis of all cell types, and CD13 may regulate availability of additional receptors or play other functions in membrane organization. Last, although we have

shown physiologic roles for CD13-mediated cell adhesion in inflammatory myeloid cell trafficking (13, 15, 19, 61) and satellite stem cell self-renewal (16, 62), we have not addressed whether its regulation of integrin availability contributes to these processes. Therefore, further investigation of CD13 in these essential intracellular processes and their potential physiological consequences is warranted.

MATERIALS AND METHODS

Cell culture

Human cervical cancer epithelial cells, C33A (passages 5 to 15) purchased from the American Type Culture Collection, were maintained in Dulbecco's modified Eagle's medium (DMEM) supplemented with 10% fetal bovine serum (FBS), 1% penicillin/streptomycin (P/S)

at 37°C, and 5% CO₂. KS KS1767 cells (passages 5 to 12) were obtained and cultured as described previously (22). Briefly, KS7167 cells were maintained in MEM supplemented with 10% FBS, 5 mM L-glutamine, 0.1 mM nonessential amino acids, 1 mM sodium pyruvate, 1× vitamins, and 1% P/S at 37°C and 5% CO₂.

Generation of CD13^{KO} KS1767 KS cells by CRISPR-Cas9 gene editing

Guide RNA were designed to specifically cut in the first exon of *CD13* gene in the human genome, Ensembl sequences ENSG00000166825. Oligos containing the guide RNA sequence were cloned into lentiCRISPR v2 (Addgene plasmid no. 52961) (63). Scrambled guide RNA was also designed as control. Guide RNAs used were as follows: 5'-CAGTGCATGATTGTGACA-3' for HCD13 and 5'-CAGTCGGCGTCATCATGAT-3' scramble control. Lentivirus was made using the packaging plasmids psPAX2 and pMD2.G (Addgene plasmid nos. 12260 and 12259) into HEK293T (Human Embryonic Kidney 293 cells expressing large T antigen) cells using Lipofectamine 2000 (Thermo Fisher Scientific). Virus was harvested at 48 hours after transfection. Human cell lines were plated and transduced by the lentivirus. Forty-eight hours after transduction, puromycin (2 ng/μl) was added to the culture to select for lentiCRISPR integration. The region of CRISPR binding was amplified by PCR and sequenced by Sanger sequencing. Clones that were shown to have frameshifts on both alleles were expanded, confirmed, and tested further to confirm the knockout of *CD13* by immunoblot and flow cytometry analysis. Plasmid pcDNA3 HA-tagged dominant-negative ARF6 T27N plasmid was purchased from Addgene. The membrane-permeant, myristoylated peptide that mimics the N terminus of ARF6, ARF6 inhibitory peptide (myr-ARF6 peptide), was purchased from MyBioSource.

Animals

Global WT and CD13^{KO} mice (C57BL/6 J strain) generated in our laboratory were housed in animal facilities at the University of Connecticut Health Center, and all experiments were performed in accordance with a protocol approved by the Institutional Animal Care and Use Committee.

Antibodies

Antibodies to paxillin [rabbit polyclonal (poly) Ab; Abcam, ab2264], phalloidin-tetramethyl rhodamine isothiocyanate (Sigma, P1951), tubulin (rat mAb; Millipore, MAB1864), actinin (mouse mAb; Abcam, ab18061), talin (rabbit poly Ab; Abcam, ab71333), β1 integrin [mouse mAb (Abcam, clone 12G10, ab30394) and rat mAb (BD Biosciences, clone 9EG7, 553715)], MB1.2 (rat mAb; Millipore, MAB1997), Rab5 (rabbit mAb; Cell Signaling Technology, 3547), Rab11 (rabbit poly Ab; Thermo Fisher Scientific, 71-5300), Rab7 (rabbit poly Ab; Thermo Fisher Scientific, PA5-22959), IQGAP1 [mouse mAb; BD Biosciences, 610612) and rabbit poly Ab (Abcam, ab86064)], ARF6 (rabbit poly Ab; Cell Signaling Technology, 3546), HA (mouse mAb; Sigma, H9658), E-cadherin (rabbit mAb; Cell Signaling Technology, 3195), GAPDH-peroxidase (mouse mAb; Sigma, G9295), EFA6 (rabbit poly Ab; Atlas Antibodies, HPA059237), EFA6 (rabbit poly Ab; Thermo Fisher Scientific, PA5-31153), and ARNO (goat poly Ab; Sigma, SAB2500109) were purchased, as stated for each above.

Retroviral vector construction and infection

Full-length HCD13 complementary DNA (cDNA) was cloned into pcDNA/V5/GW/D-TOPO (Invitrogen, San Diego, CA). The V5-

tagged CD13 was then excised and cloned into the retroviral expression vector pBM-IRES-Puro to obtain C33A-EV- or C33A-HCD13-expressing cells (15). Mutation of HCD13 Tyr⁶ to phenylalanine (Y6F) was performed as described previously (15). Cells were routinely cultured in DMEM supplemented with 10% heat-inactivated FBS, 1% P/S, L-glutamine, and glucose (4.5 g/liter) in the presence of puromycin (1 μg/ml). After the above procedure, C33A cells expressing T27N and EV or HCD13 or Y6F were generated.

Isolation of MEFs

MEFs from WT and CD13^{KO} mice were generated as described (64). MEFs were cultured in DMEM supplemented with 10% inactivated FBS, 1% P/S, L-glutamine, and glucose (4.5 g/liter).

Flow cytometry

Cells (0.5 × 10⁶) were fixed with 2% paraformaldehyde, permeabilized with 0.1% Triton X-100, and blocked with 5% bovine serum albumin (BSA) for 1 hour. Cells were stained with primary antibody mouse anti-HCD13 (452; 1:500) or rat anti-mouse β1 integrin (9EG7; 1 μg/ml) or rabbit poly antibody (12G10; 1 μg/ml) or rat anti-mouse β1 integrin antibody (MB1.2; 1 μg/ml) at 4°C for 30 min followed by secondary goat anti-mouse Alexa fluor 488 Ab (1:5000) or rabbit anti-mouse Alexa fluor 488 Ab (1:5000) at 4°C for 30 min. Flow cytometry was performed on live cells using LSRII (BD Biosciences), and the data were analyzed with FlowJo software (Tree Star).

Quantitative RT-PCR analysis

RNA was isolated using TRIzol according to the manufacturer's instructions (Invitrogen). GAPDH was used as internal control gene. Sequences of PCR primers are as follows: β1 integrin (*ITGB1*), 5'-GAAGGGTTGCCCTCCAGA-3' (forward) and 5'-GCTTGAGCTTCTCTGCTGTT-3' (reverse); *GAPDH*, 5'-GGATTGGTTCGTATTGGG-3' (forward) and 5'-GGAAGATGGTGTGGGATT-3' (reverse).

Western blotting

Cell lysates were prepared in 1% NP-40 lysis buffer containing 1× cComplete, Mini, EDTA-free Protease Inhibitor Cocktail (Roche, catalog no. 11836153001). Protein concentration was quantified using Pierce BCA Protein Assay Kit (Thermo Fisher Scientific, catalog no. 23225). Western blot samples were separated by SDS-polyacrylamide gel electrophoresis (SDS-PAGE) and transferred to nitrocellulose membranes. The nitrocellulose membranes were blocked in 1× TBST (tris-buffered saline, 0.1% Tween 20) containing 5% BSA for 1 hour followed by incubation in primary antibody in blocking buffer overnight at 4°C. Blots were washed three times in 1× TBST for 5 min each, followed by incubation at room temperature for 1 hour in blocking solution containing appropriate secondary antibody (1:5000). Membranes were washed three times in 1× TBST and developed using Clarity Max Western ECL Substrate (Bio-Rad, catalog no. 1705062) and imaged by ChemiDoc MP Imaging System (Bio-Rad). GAPDH or E-cadherin was used as loading controls.

Coimmunoprecipitation

Cell lysate (500 μg) was mixed with 5 μg of control IgG or CD13 mAb 452 overnight at 4°C with constant rotation, and proteins were immunoprecipitated with protein G-conjugated agarose beads (Invitrogen) by constant rotation for 2 hours at 4°C. The beads were washed four times in 1% NP-40 buffer containing protease and phosphatase

inhibitors, and the precipitated protein was analyzed by immunoblot using anti-IQGAP1, anti-ARF6, or anti-EFA6 antibodies.

ARF6 pull-down activation assay

ARF6 activity was measured using the bead pull-down method according to the manufacturer's instructions (Cytoskeleton Inc). Briefly, C33A cells expressing EV, Y6F, or Y6F were seeded on FN, cell-ECM adhesion was allowed to proceed for 0 to 90 min, and cells were lysed and immediately incubated with beads conjugated with the PBD of the effector GGA3 protein, which specifically binds to the active form of ARF6, ARF6-GTP. For ARF6-GTP activity bound to CD13, lysates were mixed with 5 μ g of control IgG or CD13 mAb 452 for 1 hour at 4°C, immunoprecipitated with protein G-conjugated agarose beads, eluted, and subjected to pull-down assay. The lysates were incubated with the beads, rotating at 4°C for 1 hour. The GGA3-PBD beads and bound proteins were centrifuged at 5000g at 4°C for 2 min and washed twice. After the final centrifugation, beads were resuspended in 2 \times Laemmli sample buffer and boiled for 2 min, and proteins were analyzed by SDS-PAGE and Western blot analysis using an ARF6-specific antibody provided in the kit.

Immunofluorescence analysis

Cells were grown on coverslips and serum-starved for 2 hours in plain DMEM. Cells were fixed in 4% paraformaldehyde solution for 30 min at room temperature, permeabilized with 0.1% Triton X-100 in phosphate-buffered saline (PBS) for 5 min at room temperature, washed, and blocked with normal donkey serum or 5% BSA for 1 hour at room temperature, followed by primary Ab (1:500) in 5% BSA/PBS, overnight at 4°C. The cells were washed and treated with secondary Ab (1:1200) for 1 hour at room temperature. All antibody dilutions were made in 5% BSA/PBS. For all colocalization studies, staining was performed sequentially, followed by treatment with TO-PRO-3 or DAPI (nuclear stain), mounted with ProLong Gold antifade mounting medium (Life Technologies), and analyzed by a Zeiss Axiovert fluorescence confocal microscope. Specimens were visualized at the excitation wavelength of 488 nm for Alexa 488, 543 nm for Alexa 594, 405 nm for DAPI, and 633 nm for TO-PRO-3. Images were photographed with a Zeiss LSM 880 microscope using the Zeiss Achroplan 63 \times or 100 \times oil objectives. Images were analyzed by LSM software (Zeiss) and quantified by MetaMorph software (Molecular Devices).

Pulse-chase experiments

Cells were serum-starved for 2 hours at 37°C in DMEM/0.5% BSA and stained with unlabeled mAbs detecting either murine β 1 integrin (BD Biosciences, clone 9EG7) or human β 1 integrin (Abcam, clone 12G10) at 5 μ g/ml in DMEM/0.5% BSA on ice for 30 min (surface binding). Cells were transferred to 37°C for 1 hour to allow internalization (pulse). After pulse, cells were briefly acid-rinsed in 0.5% acetic acid and 0.5 M NaCl (pH 3.0) for 45 s to remove noninternalized and surface-bound antibodies. Cells for pulse-only conditions were either fixed (surface β 1 integrin) or fixed and permeabilized (internalized β 1 integrin). Cells undergoing chase were chased in antibody-free complete medium for 2 or 4 hours at 37°C to assess receptor recycling back to the surface (Chase/2h or Chase/4h), and cells were fixed or fixed/permeabilized. The remaining β 1 integrin mAbs in pulse-only and pulse/chase conditions were detected by with an FITC-labeled secondary antibody and measured by IF or flow cytometry. Cells were exposed to 25 μ M of the myristoylated ARF6 2-13 peptide or vehicle before assay.

Capture ELISA

To assess internalization of integrin, serum-starved WT and CD13^{KO} MEFs or WT KS and CD13 CRISPR KS cells were surface-labeled with NHS-S-Biotin (0.2 mg/ml; Pierce) at 4°C for 30 min. Labeled cells were washed in cold PBS, and internalization was allowed to proceed at 37°C for the times indicated in the figures, at which point the remaining surface biotin was removed by treatment with 20 mM MesNa in 50 mM tris-HCl (pH 8.6) and 100 mM NaCl for 15 min at 4°C. MesNa was quenched by iodoacetamide (20 mM) treatment. Cells were lysed in radioimmunoprecipitation assay lysis buffer containing a protease inhibitor cocktail, and the amount of internalized β 1 integrin was quantified. Cell lysate was normalized to total protein concentration, and amount of biotinylated integrin was determined by capture ELISA (20). Briefly, 96-well microtiter plates were coated with 9EG7 (5 μ g/ml; MEFs) or 12G10 (KS1767) in 0.05 M sodium carbonate (pH 9.6) at 4°C. Plates were blocked in PBS containing 5% BSA at room temperature for 1 hour. Captured integrin was measured by overnight incubation of cell lysate (100 μ g) at 4°C. Plates were washed in PBS/Tween-20 and incubated with streptavidin-HRP for 1 hour at 4°C, and biotinylated integrin was measured by addition of a chromogenic agent ortho-phenylenediamine. Internalized integrin was represented as a percentage of the initial surface integrin pool measured in cells without MesNa treatment at time 0 min.

To determine integrin recycling, cells were surface biotin-labeled, and internalization was allowed to proceed during a period of unperturbed incubation for 30 min. Following removal with MesNa, cells were chased in complete medium at 37°C for the times indicated in the figures. At each harvest point, biotin was eliminated from the surface by a second round of MesNa treatment to exclude integrins that had recycled back to the surface, and the level of biotinylated integrin remaining in the cells (internalized) was measured in cell lysates by capture ELISA. The amount of recycled integrin is based on the assumption that (% internal + % recycled = 100%) and calculated as the difference between time 0 min (maximal internalization) and the relative amount of integrin remaining in the cell at each subsequent chase point or $100\% - \% \text{ internalized at chase (internal at time } x/\text{max internal time } 0 \times 100) = \% \text{ recycled}$.

Cell-ECM adhesion

The cell-ECM adhesion assay was performed as described previously (65). Briefly, either MEFs pretreated with anti-mouse CD13 antibody (SL13) or C33A cells were washed in DMEM/Hepes medium and allowed to adhere to microtiter plate for 0 to 1 hour at 37°C. Before seeding, the microtiter plates were coated with FN (Millipore, FC010) for overnight at 4°C, followed by blocking with heat-inactivated BSA at room temperature for 1 hour. Nonadherent cells were removed by gentle aspiration and washing followed by fixation with 5% glutaraldehyde for 20 min at room temperature. Cells were stained with 0.1% crystal violet and 200 mM MES [2-(N-morpholino)ethanesulfonic acid] (pH 6.0) for 1 hour at room temperature, dye was solubilized in 10% acetic acid, and absorbance was measured at 595 nm using a plate reader (Bio-Rad).

Cell spreading

The cell spreading assay was performed as described previously (65). Briefly, MEFs or C33A cells at a density of 1×10^5 cells/ml were seeded onto coverslips that were coated with FN and blocked with BSA, as described in the adhesion assay, for 0 to 1 hour at 37°C.

Cells were stained with the primary antibody recognizing the focal adhesion protein paxillin, followed by Alexa 488–conjugated secondary antibody. The relative area of spreading was determined by measuring the area circumscribed by paxillin staining and quantitated using Fiji software. Cells of similar nuclear size were used for measurement.

Cell migration

The cell migration assay was performed as described previously (66). Briefly, a subconfluent monolayer of MEFs or C33A cells at a density of 5×10^5 cells/ml were spread onto coverslips that were coated with FN and blocked with BSA as described in the adhesion assay. A scratch was created with a P20 pipette tip, the monolayer was washed to remove debris, and cells were left to close the wound for 0 to 6 hours at 37°C in complete growth medium. At the indicated times, cells were fixed with 4% PFA (paraformaldehyde), stained with crystal violet and imaged using phase-contrast microscopy. In MEF cell cultures, the number of cells migrating into the wound area was counted, whereas in C33A cell cultures, the distance traveled by the leading front over time was measured.

Plasma membrane isolation

Plasma membrane fraction from whole-cell lysate was isolated using the Minute Plasma Membrane Protein Isolation Kit according to the manufacturer's instructions (Invent Biotechnologies, SM-005-P). Briefly, whole-cell lysates were prepared in buffer A (provided by the manufacturer) by vortexing three times for 5 s each and incubating on ice for 20 min followed by centrifugation at 700g for 1 min to separate pellet containing nuclei and larger debris. The supernatant was transferred to a fresh microfuge tube and centrifuged at 4°C for 1 hour at 16,000g. The supernatant containing the cytosolic fraction was transferred to a new tube, and the pellet containing total membrane fraction (organelle membrane and plasma membrane) was isolated. For isolation of plasma membrane fraction from total membrane fraction, the pellet containing total membrane fraction was thoroughly resuspended in 200 ml of buffer B (provided by the manufacturer) by repeated pipetting followed by centrifugation at 8000g for 20 min at 4°C. The pellet containing organelle membrane proteins was isolated. The supernatant was transferred to a fresh microfuge tube to which 1.6 ml of cold $1 \times$ PBS was added, mixed, and centrifuged at 16,000g for 1 hour. The pellet containing plasma membrane proteins was resuspended in Minute Denaturing Protein Solubilization reagent (provided by the manufacturer) for SDS-PAGE and immunoblot analysis. Purity was verified by positive expression of E-cadherin but negative expression of early endosome antigen 1.

Statistical analysis

Results are presented as means \pm SD. Statistical analysis was performed using unpaired, two-tailed Student's *t* test using GraphPad Prism. Differences were considered significant at $P \leq 0.05$.

SUPPLEMENTARY MATERIALS

stke.sciencemag.org/cgi/content/full/12/579/eaav5938/DC1

Fig. S1. CD13 is necessary for cell spreading and migration.

Fig. S2. Illustration of the $\beta 1$ integrin mAb-induced pulse-chase assay.

Fig. S3. Equivalent surface abundance of MB1.2 in WT and CD13^{KO} MEFs.

Fig. S4. Impaired cell adhesion, migration, and $\beta 1$ integrin recycling in CD13 CRISPR human KS cells.

Fig. S5. Aluminum fluoride treatment led to actin-rich protrusions in C33A-HCD13 cells.

REFERENCES AND NOTES

1. M. Vicente-Manzanares, A. R. Horwitz, Adhesion dynamics at a glance. *J. Cell Sci.* **124**, 3923–3927 (2011).
2. A. J. Ridley, M. A. Schwartz, K. Burridge, R. A. Firtel, M. H. Ginsberg, G. Borisy, J. T. Parsons, A. R. Horwitz, Cell migration: Integrating signals from front to back. *Science* **302**, 1704–1709 (2003).
3. N. De Franceschi, H. Hamidi, J. Alanko, P. Sahgal, J. Ivaska, Integrin traffic—the update. *J. Cell Sci.* **128**, 839–852 (2015).
4. J. Cherfils, M. Zeghouf, Regulation of small GTPases by GEFs, GAPs, and GDIs. *Physiol. Rev.* **93**, 269–309 (2013).
5. S. Hanna, M. El-Sibai, Signaling networks of rho GTPases in cell motility. *Cell. Signal.* **25**, 1955–1961 (2013).
6. J. K. Schweitzer, A. E. Sedgwick, C. D'Souza-Schorey, ARF6-mediated endocytic recycling impacts cell movement, cell division and lipid homeostasis. *Semin. Cell Dev. Biol.* **22**, 39–47 (2011).
7. B. Hu, B. Shi, M. J. Jarzynka, J.-J. Yiin, C. D'Souza-Schorey, S.-Y. Cheng, ADP-ribosylation factor 6 regulates glioma cell invasion through the IQ-domain GTPase-activating protein 1-Rac1-mediated pathway. *Cancer Res.* **69**, 794–801 (2009).
8. A. M. Powelka, J. Sun, J. Li, M. Gao, L. M. Shaw, A. Sonnenberg, V. W. Hsu, Stimulation-dependent recycling of integrin $\beta 1$ regulated by ARF6 and Rab11. *Traffic* **5**, 20–36 (2004).
9. P. D. Allaire, M. Seyed Sadr, M. Chaineau, E. Seyed Sadr, S. Konefal, M. Fotouhi, D. Maret, B. Ritter, R. F. Del Maestro, P. S. McPherson, Interplay between Rab35 and Arf6 controls cargo recycling to coordinate cell adhesion and migration. *J. Cell Sci.* **126**, 722–731 (2013).
10. Y. Onodera, J.-M. Nam, A. Hashimoto, J. C. Norman, H. Shirato, S. Hashimoto, H. Sabe, Rab5c promotes AMAP1-PRKD2 complex formation to enhance $\beta 1$ integrin recycling in EGF-induced cancer invasion. *J. Cell Biol.* **197**, 983–996 (2012).
11. N. Petrovic, W. Schacke, J. R. Gahagan, C. A. O'Connor, B. Winnicka, R. E. Conway, P. Mina-Osorio, L. H. Shapiro, CD13/APN regulates endothelial invasion and filopodia formation. *Blood* **110**, 142–150 (2007).
12. M. Ghosh, B. McAuliffe, J. Subramani, S. Basu, L. H. Shapiro, CD13 regulates dendritic cell cross-presentation and T cell responses by inhibiting receptor-mediated antigen uptake. *J. Immunol.* **188**, 5489–5499 (2012).
13. M. Ghosh, J. Subramani, M. M. Rahman, L. H. Shapiro, CD13 restricts TLR4 endocytic signal transduction in inflammation. *J. Immunol.* **194**, 4466–4476 (2015).
14. P. Mina-Osorio, L. H. Shapiro, E. Ortega, CD13 in cell adhesion: Aminopeptidase N (CD13) mediates homotypic aggregation of monocytic cells. *J. Leukoc. Biol.* **79**, 719–730 (2006).
15. J. Subramani, M. Ghosh, M. M. Rahman, L. A. Caromile, C. Gerber, K. Rezaul, D. K. Han, L. H. Shapiro, Tyrosine phosphorylation of CD13 regulates inflammatory cell-cell adhesion and monocyte trafficking. *J. Immunol.* **191**, 3905–3912 (2013).
16. M. M. Rahman, M. Ghosh, J. Subramani, G.-H. Fong, M. E. Carlson, L. H. Shapiro, CD13 regulates anchorage and differentiation of the skeletal muscle satellite stem cell population in ischemic injury. *Stem Cells* **32**, 1564–1577 (2014).
17. M. Ghosh, C. Gerber, M. M. Rahman, K. M. Vernier, F. E. Pereira, J. Subramani, L. A. Caromile, L. H. Shapiro, Molecular mechanisms regulating CD13-mediated adhesion. *Immunology* **142**, 636–647 (2014).
18. S. V. Bhagwat, N. Petrovic, Y. Okamoto, L. H. Shapiro, The angiogenic regulator CD13/APN is a transcriptional target of Ras signaling pathways in endothelial morphogenesis. *Blood* **101**, 1818–1826 (2003).
19. P. Mina-Osorio, B. Winnicka, C. O'Connor, C. L. Grant, L. K. Vogel, D. Rodriguez-Pinto, K. V. Holmes, E. Ortega, L. H. Shapiro, CD13 is a novel mediator of monocytic/endothelial cell adhesion. *J. Leukoc. Biol.* **84**, 448–459 (2008).
20. E. Argenzio, C. Margadant, D. Leyton-Puig, H. Janssen, K. Jalink, A. Sonnenberg, W. H. Moolenaar, CLIC4 regulates cell adhesion and $\beta 1$ integrin trafficking. *J. Cell Sci.* **127**, 5189–5203 (2014).
21. N. Petrovic, S. V. Bhagwat, W. J. Ratzan, M. C. Ostrowski, L. H. Shapiro, CD13/APN transcription is induced by RAS/MAPK-mediated phosphorylation of Ets-2 in activated endothelial cells. *J. Biol. Chem.* **278**, 49358–49368 (2003).
22. S. V. Bhagwat, J. Lahdenranta, R. Giordano, W. Arap, R. Pasqualini, L. H. Shapiro, CD13/APN is activated by angiogenic signals and is essential for capillary tube formation. *Blood* **97**, 652–659 (2001).
23. P.-W. Chen, R. Luo, X. Jian, P. A. Randazzo, The Arf6 GTPase-activating proteins ARAP2 and ACAP1 define distinct endosomal compartments that regulate integrin $\alpha 5 \beta 1$ traffic. *J. Biol. Chem.* **289**, 30237–30248 (2014).
24. S. Christoforidis, H. M. McBride, R. D. Burgoyne, M. Zerial, The Rab5 effector EEA1 is a core component of endosome docking. *Nature* **397**, 621–625 (1999).
25. J. Noritake, T. Watanabe, K. Sato, S. Wang, K. Kaibuchi, IQGAP1: A key regulator of adhesion and migration. *J. Cell Sci.* **118**, 2085–2092 (2005).
26. S. C. Mateer, A. E. McDaniel, V. Nicolas, G. M. Habermacher, M.-J. S. Lin, D. A. Cromer, M. E. King, G. S. Bloom, The mechanism for regulation of the F-actin binding activity of IQGAP1 by calcium/calmodulin. *J. Biol. Chem.* **277**, 12324–12333 (2002).

27. G. Jacquemet, M. J. Humphries, IQGAP1 is a key node within the small GTPase network. *Small GTPases* **4**, 199–207 (2013).
28. N. R. Paul, G. Jacquemet, P. T. Caswell, Endocytic trafficking of integrins in cell migration. *Curr. Biol.* **25**, R1092–R1105 (2015).
29. J. L. Dunphy, R. Moravec, K. Ly, T. K. Lasell, P. Melancon, J. E. Casanova, The Arf6 GEF GEP100/BRAG2 regulates cell adhesion by controlling endocytosis of $\beta 1$ integrins. *Curr. Biol.* **16**, 315–320 (2006).
30. M. R. Morgan, H. Hamidi, M. D. Bass, S. Warwood, C. Ballestrem, M. J. Humphries, Syndecan-4 phosphorylation is a control point for integrin recycling. *Dev. Cell* **24**, 472–485 (2013).
31. L. A. Cohen, A. Honda, P. Varnai, F. D. Brown, T. Balla, J. G. Donaldson, Active Arf6 recruits ARNO/cytohesin GEFs to the PM by binding their PH domains. *Mol. Biol. Cell* **18**, 2244–2253 (2007).
32. C. T. Davis, W. Zhu, C. C. Gibson, J. A. Bowman-Kirigin, L. Sorensen, J. Ling, H. Sun, S. Navankasattusas, D. Y. Li, ARF6 inhibition stabilizes the vasculature and enhances survival during endotoxic shock. *J. Immunol.* **192**, 6045–6052 (2014).
33. W. Choi, Z. A. Karim, S. W. Whiteheart, Arf6 plays an early role in platelet activation by collagen and convulxin. *Blood* **107**, 3145–3152 (2006).
34. A. Ruiz-Sánchez, L. Kremer, M. A. Alonso, J. Millán, I. Correas, Protein 4.1R regulates cell migration and IQGAP1 recruitment to the leading edge. *J. Cell Sci.* **124**, 2529–2538 (2011).
35. H. Radhakrishna, R. D. Klausner, J. G. Donaldson, Aluminum fluoride stimulates surface protrusions in cells overexpressing the ARF6 GTPase. *J. Cell Biol.* **134**, 935–947 (1996).
36. R. Eva, S. Crisp, J. R. K. Marland, J. C. Norman, V. Kanamarlapudi, C. French-Constant, J. W. Fawcett, ARF6 directs axon transport and traffic of integrins and regulates axon growth in adult DRG neurons. *J. Neurosci.* **32**, 10352–10364 (2012).
37. S. J. Oh, L. C. Santy, Differential effects of cytohesins 2 and 3 on $\beta 1$ integrin recycling. *J. Biol. Chem.* **285**, 14610–14616 (2010).
38. S. Frank, S. Upender, S. H. Hansen, J. E. Casanova, ARNO is a guanine nucleotide exchange factor for ADP-ribosylation factor 6. *J. Biol. Chem.* **273**, 23–27 (1998).
39. V. Kanamarlapudi, Exchange factor EFA6R requires C-terminal targeting to the plasma membrane to promote cytoskeletal rearrangement through the activation of ADP-ribosylation factor 6 (ARF6). *J. Biol. Chem.* **289**, 33378–33390 (2014).
40. M. Franco, P. J. Peters, J. Boretto, E. van Donselaar, A. Neri, C. D'Souza-Schorey, P. Chavrier, EFA6, a sec7 domain-containing exchange factor for ARF6, coordinates membrane recycling and actin cytoskeleton organization. *EMBO J.* **18**, 1480–1491 (1999).
41. S. D. Conner, S. L. Schmid, Regulated portals of entry into the cell. *Nature* **422**, 37–44 (2003).
42. R. E. Bridgewater, J. C. Norman, P. T. Caswell, Integrin trafficking at a glance. *J. Cell Sci.* **125**, 3695–3701 (2012).
43. T. Zech, S. D. J. Calaminus, P. Caswell, H. J. Spence, M. Carnell, R. H. Insall, J. Norman, L. M. Machesky, The Arp2/3 activator WASH regulates $\alpha 5 \beta 1$ -integrin-mediated invasive migration. *J. Cell Sci.* **124**, 3753–3759 (2011).
44. R. T. Bottcher, C. Stremmel, A. Meves, H. Meyer, M. Widmaier, H.-Y. Tseng, R. Fässler, Sorting nexin 17 prevents lysosomal degradation of $\beta 1$ integrins by binding to the $\beta 1$ -integrin tail. *Nat. Cell Biol.* **14**, 584–592 (2012).
45. C. D. White, H. H. Erdemir, D. B. Sacks, IQGAP1 and its binding proteins control diverse biological functions. *Cell. Signal.* **24**, 826–834 (2012).
46. A. C. Hedman, J. M. Smith, D. B. Sacks, The biology of IQGAP proteins: Beyond the cytoskeleton. *EMBO Rep.* **16**, 427–446 (2015).
47. P. Mina-Osorio, E. Ortega, Aminopeptidase N (CD13) functionally interacts with Fc γ R in human monocytes. *J. Leukoc. Biol.* **77**, 1008–1017 (2005).
48. M. I. Villaseñor-Cardoso, D. A. Frausto-Del-Río, E. Ortega, Aminopeptidase N (CD13) is involved in phagocytic processes in human dendritic cells and macrophages. *Biomed. Res. Int.* **2013**, 562984 (2013).
49. I. Licona-Limón, C. A. Garay-Canales, O. Muñoz-Paletta, E. Ortega, CD13 mediates phagocytosis in human monocytic cells. *J. Leukoc. Biol.* **98**, 85–98 (2015).
50. L. K. Vogel, M. Spiess, H. Sjöström, O. Norén, Evidence for an apical sorting signal on the ectodomain of human aminopeptidase N. *J. Biol. Chem.* **267**, 2794–2797 (1992).
51. L. K. Vogel, O. Norén, H. Sjöström, The apical sorting signal on human aminopeptidase N is not located in the stalk but in the catalytic head group. *FEBS Lett.* **308**, 14–17 (1992).
52. A. Buehler, M. A. M. J. van Zandvoort, B. J. Stelt, T. M. Hackeng, B. H. G. J. Schrans-Stassen, A. Bennaghmouch, L. Hofstra, J. P. M. Cleutjens, A. Duijvestijn, M. B. Smeets, D. P. V. de Kleijn, M. J. Post, E. D. de Muinck, cNGR: A novel homing sequence for CD13/APN targeted molecular imaging of murine cardiac angiogenesis in vivo. *Arterioscler. Thromb. Vasc. Biol.* **26**, 2681–2687 (2006).
53. D. T. Brandt, S. Marion, G. Griffiths, T. Watanabe, K. Kaibuchi, R. Grosse, Dia1 and IQGAP1 interact in cell migration and phagocytic cup formation. *J. Cell Biol.* **178**, 193–200 (2007).
54. M. Yamaoka-Tojo, M. Ushio-Fukai, L. Hilenski, S. I. Dikalov, Y. E. Chen, T. Tojo, T. Fukai, M. Fujimoto, N. A. Patrushev, N. Wang, C. D. Kontos, G. S. Bloom, R. W. Alexander, IQGAP1, a novel vascular endothelial growth factor receptor binding protein, is involved in reactive oxygen species—Dependent endothelial migration and proliferation. *Circ. Res.* **95**, 276–283 (2004).
55. G. S. Bogatkevich, A. Ludwicka-Bradley, C. B. Singleton, J. R. Bethard, R. M. Silver, Proteomic analysis of CTGF-activated lung fibroblasts: Identification of IQGAP1 as a key player in lung fibroblast migration. *Am. J. Physiol. Lung Cell. Mol. Physiol.* **295**, L603–L611 (2008).
56. S. P. Amarachintha, K. J. Ryan, M. Cayer, N. S. Boudreau, N. M. Johnson, C. A. Heckman, Effect of Cdc42 domains on filopodia sensing, cell orientation, and haptotaxis. *Cell. Signal.* **27**, 683–693 (2015).
57. G. Izumi, T. Sakisaka, T. Baba, S. Tanaka, K. Morimoto, Y. Takai, Endocytosis of E-cadherin regulated by Rac and Cdc42 small G proteins through IQGAP1 and actin filaments. *J. Cell Biol.* **166**, 237–248 (2004).
58. A. Sakurai, X. Jian, C. J. Lee, Y. Manavski, E. Chavakis, J. Donaldson, P. A. Randazzo, J. S. Gutkind, Phosphatidylinositol-4-phosphate 5-kinase and GEP100/Brag2 protein mediate antiangiogenic signaling by semaphorin 3E-plexin-D1 through Arf6 protein. *J. Biol. Chem.* **286**, 34335–34345 (2011).
59. H. Sakagami, T. Honma, J. Sukegawa, Y. Owada, T. Yanagisawa, H. Kondo, Somatodendritic localization of EFA6A, a guanine nucleotide exchange factor for ADP-ribosylation factor 6, and its possible interaction with alpha-actinin in dendritic spines. *Eur. J. Neurosci.* **25**, 618–628 (2007).
60. J. Milanini, R. Fayad, M. Partisani, P. Lecine, J.-P. Borg, M. Franco, F. Luton, EFA6 proteins regulate lumen formation through α -actinin 1. *J. Cell Sci.* **131**, jcs209361 (2018).
61. F. E. Pereira, C. Cronin, M. Ghosh, S.-Y. Zhou, M. Agosto, J. Subramani, R. Wang, J.-B. Shen, W. Schacke, B. Liang, T. H. Yang, B. McAulliffe, B. T. Liang, L. H. Shapiro, CD13 is essential for inflammatory trafficking and infarct healing following permanent coronary artery occlusion in mice. *Cardiovasc. Res.* **100**, 74–83 (2013).
62. M. M. Rahman, J. Subramani, M. Ghosh, J. K. Denninger, K. Takeda, G.-H. Fong, M. E. Carlson, L. H. Shapiro, CD13 promotes mesenchymal stem cell-mediated regeneration of ischemic muscle. *Front. Physiol.* **4**, 402 (2014).
63. N. E. Sanjana, O. Shalem, F. Zhang, Improved vectors and genome-wide libraries for CRISPR screening. *Nat. Methods* **11**, 783–784 (2014).
64. L. C. Samuelson, J. M. Metzger, Isolation and freezing of primary mouse embryonic fibroblasts (MEF) for feeder plates. *CSH Protoc.* **2006**, pdb.prot4485 (2006).
65. M. J. Humphries, Cell adhesion assays. *Methods Mol. Biol.* **522**, 203–210 (2009).
66. C.-C. Liang, A. Y. Park, J.-L. Guan, In vitro scratch assay: A convenient and inexpensive method for analysis of cell migration in vitro. *Nat. Protoc.* **2**, 329–333 (2007).

Acknowledgments: We thank L. Caromile (Center for Vascular Biology) for providing the lentivirus and assistance with the retroviral-based cloning and expression system. We also thank S. Staurovsky (Center for Cell Analysis and Modeling) and C. Stoddard (Human Genome Editing Core at UConn Health) for technical services. **Funding:** This work was supported by NIH grants R01HL127449 and R01HL125186 (to L.H.S. and M.G.). **Author contributions:** M.G. and L.H.S. conceptualized the study. M.G., R.L., and L.H.S. crafted the methodology. M.G., R.L., C.D., I.L., and B.A. performed the investigations. All authors performed the formal analysis. M.G. wrote the original draft. C.D., B.A., M.G., and L.H.S. revised and edited the manuscript. M.G. and L.H.S. supervised the study, obtained the resources, and acquired the funding. **Competing interests:** The authors declare a potential conflict of interest in that the mAb SL-13 is licensed to EMD-Millipore by L.H.S. All other authors declare they have no competing financial interests. **Data and materials availability:** All data needed to evaluate the conclusions in the paper are present in the paper or the Supplementary Materials.

Submitted 2 October 2018
Accepted 12 April 2019
Published 30 April 2019
10.1126/scisignal.aav5938

Citation: M. Ghosh, R. Lo, I. Ivic, B. Aguilera, V. Qendro, C. Devarakonda, L. H. Shapiro, CD13 tethers the IQGAP1-ARF6-EFA6 complex to the plasma membrane to promote ARF6 activation, $\beta 1$ integrin recycling, and cell migration. *Sci. Signal.* **12**, eaav5938 (2019).

CD13 tethers the IQGAP1-ARF6-EFA6 complex to the plasma membrane to promote ARF6 activation, β 1 integrin recycling, and cell migration

Mallika Ghosh, Robin Lo, Ivan Ivic, Brian Aguilera, Veneta Qendro, Charan Devarakonda and Linda H. Shapiro

Sci. Signal. **12** (579), eaav5938.
DOI: 10.1126/scisignal.aav5938

Recycle and go forth!

Cell migration and motility are critical to embryonic development, immunity, and tissue repair, but uncontrolled migration can lead to disease. Cell migration is mediated in large part through mechanical signals from the cell surface, such as those mediated through the cyclic trafficking of integrins in response to contact with the extracellular matrix (ECM). Ghosh *et al.* found that the presence of the multifunctional peptidase CD13 at the cell surface facilitated the recruitment of a complex of proteins to the leading edge of migrating cells that promoted β 1 integrin recycling to the surface, rather than its degradation, after ECM contact-induced internalization, which enhanced cell migration. These findings expand our understanding of cell migration mechanisms and identify possible targets to therapeutically control it.

ARTICLE TOOLS	http://stke.sciencemag.org/content/12/579/eaav5938
SUPPLEMENTARY MATERIALS	http://stke.sciencemag.org/content/suppl/2019/04/26/12.579.eaav5938.DC1
RELATED CONTENT	http://stke.sciencemag.org/content/sigtrans/11/560/eaat3178.full http://stke.sciencemag.org/content/sigtrans/11/556/eaao4354.full http://stke.sciencemag.org/content/sigtrans/11/534/eaan8799.full
REFERENCES	This article cites 66 articles, 38 of which you can access for free http://stke.sciencemag.org/content/12/579/eaav5938#BIBL
PERMISSIONS	http://www.sciencemag.org/help/reprints-and-permissions

Use of this article is subject to the [Terms of Service](#)